

Università degli Studi della Calabria

Dipartimento di Fisica

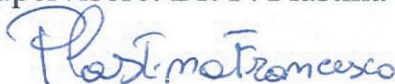
Tesi di Dottorato di Ricerca

FIS/03

Properties of Entanglement in a Spin Chain with Impurities

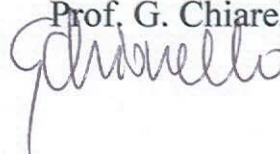
Dottorando: Dr. Tony John George Apollaro

Supervisore: Dr. F. Plastina



Coordinatore del corso di dottorato:

Prof. G. Chiarello



Contents

Introduction	ii
1 Entanglement	1
1.1 Introduction to Entanglement	1
1.2 Density Operator	3
1.2.1 Reduced Density Operator	5
1.2.2 Schmidt Decomposition	6
1.2.3 The Qubit	7
1.3 Entanglement Measures	9
1.3.1 Entropy	10
1.3.2 Mixed-State Entanglement	14
1.4 Quantum Operations	17
1.4.1 Fidelity	20
1.5 Application of Entanglement	21
1.5.1 Dense Coding	22
1.5.2 Teleportation	22
1.5.3 Quantum Key Distribution	23
1.5.4 Entanglement and Quantum Phase Transition	24
2 Spin Systems	26
2.1 Spin Hamiltonian	28
2.2 1D Spin Chain with Defects	32
2.2.1 Physical Systems Described by the Hamiltonian	33
2.3 Green's Function	36
2.4 The XX Model with One Defect	38
2.5 Ground-State Entanglement	41
2.6 Fidelity and Concurrence in our Model	42
2.7 Information Storage	46

2.7.1	Quality of the Storage	48
2.8	Quantum-State Transmission	51
2.9	Finite Size Chain	54
3	1D Spin Chain with Two Defects	58
3.1	Hamiltonian	59
3.2	Ground-State Entanglement	64
3.3	Quantum-State Transmission	66
	Conclusions	73

Introduction

In the last decades the attitude of the physics community towards non-local quantum correlations (entanglement) has experienced a deep change. From being mainly a bizarre and counter-intuitive characteristic of quantum mechanics, it has become a keyword of a deeper understanding of quantum mechanics itself, by throwing light on quantum many-body phenomena like decoherence and quantum phase transitions, just to name a few. At the same time entanglement has become the main ingredient of a new highly-interdisciplinary field: quantum information theory (QIT). In this framework entanglement has been considered a resource to accomplish various QIT tasks, otherwise inconceivable, like dense coding, teleportation and quantum information processing.

The perspective to realize powerful entanglement-based applications has directed the QIT community to search for physical systems which, with a minimal external-control operations, can perform these applications. Whatever the physical implementation, a common question of central importance is the ability to distribute with high efficiency quantum states and/or entanglement between different end-users in order to obtain meaningful experimental protocols.

The present work is based on the suggestion to use solid state systems, more precisely those described by a 1D spin- $\frac{1}{2}$ hamiltonian, both as qubit registers and coherent data bus. Much work has been carried out on 1D spin systems with various spin-spin interaction hamiltonians, achieving, e.g., both perfect quantum-state transfer and ground-state entanglement control. However, the effect of the presence of impurities, given, for example, by magnetic fields defects at some lattice point has not yet been considered in detail. Our work deals with such a system: a 1D spin- $\frac{1}{2}$ ring, i.e. a chain with periodic boundary conditions, with isotropic spin-spin Heisenberg-type interaction in a transverse magnetic field which presents local inhomogeneities. This causes

a change of the qubit energy level spacing at the impurity sites with respect to the rest of the ring's qubits. Our interest in this system is also motivated by the fact that several experimental implementations have already been realized both with cold atoms trapped in optical lattices and with Josephson junction arrays.

Exploiting the conservation of the total spin component along the z axis (the direction of the applied magnetic field), we focus on the invariant one-excitation sector of the Hilbert space, because of the importance of singlet-state transmission along the chain. In this sector our hamiltonian becomes equivalent to a tight-binding model and the exact solutions of finite-impurities hamiltonians are obtainable via the Green's operator formalism. Moreover, as even a single impurity can lead to spatial localization of the wave function, our system undergoes a quantum phase transition and a new localized ground state arises, whose entanglement content is analyzed.

We begin our work by adding a single impurity at one spin site, say l , in the ring and solve, in the thermodynamic limit, the eigenvalue problem in the one-excitation sector. We obtain that the energy spectrum of the hamiltonian, apart from the unchanged continuous energy band, exhibits a discrete energy level which can be found both above or under the energy band. The eigenstates associated to the continuous band are represented by distorted plane waves, accounting for the scattering at the impurity site. The discrete eigenstate, on the other hand, is localized around the defect, in the sense that there's an exponentially decaying probability to find the excitation, that is the reversed spin, far away from the impurity site (sec.2.4).

We find that in the paramagnetic phase, i.e. for the qubit level spacing greater than the spin exchange coupling, there exists a critical value of a parameter, named α , given by the ratio of the local inhomogeneity on site l and the exchange coupling. For α exceeding α_c the ground state becomes the discrete, localized eigenstate of the hamiltonian and a non-zero two-party entanglement, which we measure by the concurrence, arises in the new ground state. This entanglement content too shows a localized spatial structure around the impurity, and in the limit of $\alpha \gg 1$, when the localization length goes to zero, also the spatial extension of the concurrence reduces to zero, so that, in this limit, the ground state is again a factorized state (sec.2.5)

Next we turn to quantum-state transmission tasks. First we consider the situation in which a singlet state has been realized between an external spin, i.e. a spin not participating in the hamiltonian's dynamics, and another, the sender, different from the impurity. This setup has been proposed in order

to send entanglement, with possibly high efficiency, along the chain up to another spin, the receiver. This process allows to realize two-party entangled states between the external spin and an arbitrary spin of the ring; which is a necessary prerequisite of almost all quantum communication protocols, for example.

We find that entanglement propagates almost freely up to the impurity which acts like an entanglement mirror, characterized by transmission and reflection coefficients (sec.2.8). The reasons of this behaviour reside in the analytic structure of the concurrence (the two-party entanglement measure between the external spin and the receiver spin), which identifies with the amplitude of the transmission of the excitation from the sender to the receiver (sec.2.6). Therefore, the excitation propagates both through the mediation of the continuous band, where distorted plane waves affect only slightly the free entanglement's propagation, and through the mediation of the localized state, which affects the entanglement's propagation only within the localization length. With high values of the impurity strength, the latter contribution goes to zero, while the impurity qubit energy spacing has become considerable larger than that of the other qubits; as a consequence, the energy carried by the entanglement wave isn't enough to transmit the excitation at the impurity spin. Because of the conservation of the z -component of the total spin, the excitation, and the entanglement, is reflected backward.

If we instead consider the situation in which the sender identifies with the impurity, the spin ring acts as an entanglement memory (sec.2.7), in the sense that the initial entanglement doesn't diffuse away (up to second order effects in $\frac{1}{\alpha}$). Moreover, this quantum information storage effect isn't limited to the singlet state, as the relative phase of the superposition of an arbitrary maximally entangled state in the one-excitation sector is almost perfectly retained (sec.2.7.1).

Again this effect can be explained by the impossibility, in the limit $\alpha \gg 1$, of the excitation to leave the impurity site.

Then we turn to single-qubit quantum state transfer, meaning that an arbitrary state is encoded in a spin of the ring (the sender), and one wants to use the spin ring as a quantum channel to send the quantum state to another spin (the receiver). The efficiency of this transmission is measured by the fidelity, which too is proportional to the amplitude of the excitation transmission (sec.2.7). Therefore similar results are obtained: 1.) high-fidelity quantum-state storage at the impurity site; 2.) possibility to achieve quantum-state transmission control by operating on the impurity strength.

With similar motivations, we have studied the same hamiltonian with one more impurity added at another site, say m . The eigenspectrum of the hamiltonian exhibits a more complicated structure, admitting the possibility of one or two discrete energy eigenvalues. If there's only one, it can be either below or above the unchanged energy band. If the system presents two discrete eigenvalues, they can be found either both below, or both above the energy band, or one above and another below, depending on the strength of the impurities (sec.3.1). As in the one-defect model, the associated discrete eigenstates exhibit a localized spatial structure and the system undergoes a first order quantum phase transition for appropriate values of the defects. This is reflected on ground-state entanglement, which too becomes localized around the impurity sites, but notable differences arise with respect to the one-impurity model.

For large enough, and equal, defects strength the ground-state is localized around both impurity sites l and m . Therefore the system doesn't reduce to a product state, as in the one-defect model. On the contrary, the two impurities appear to be maximally entangled, independently of their distance, while the rest of the ring turns out to be in a factorized state. Furthermore, the two-party entanglement content between the qubits around one defect can be changed by acting on the defect's strength of the other spin, in the sense that a reduction of the m -qubit impurity raises the concurrence between the qubits around the other qubit l . At the same time, the concurrence in the neighbourhood of site m decreases (sec.3.2). Obviously the reversed situation is obtained if the defect's strength on site m is increased, because of the label exchange symmetry. This achieves a remote control of entanglement.

Then we analyze quantum-information transmission in our two-impurities model and consider the case in which two localized eigenstates are present in the eigenspectrum. This assumption is motivated by the observation that already for small values of the defects, the systems exhibits such an energy structure and, because of our one-defect analysis, it is in this regime that more interesting phenomena arise.

First we consider the case in which the sender is encoded in a spin different from the defects, and we find the same qualitative behaviour in terms of reflection and transmission of entanglement waves. But now we are in presence of two mirrors and, placing the sender within a region bounded by the two defects, it is possible to trap therein the entanglement waves with different results: 1.) if the sites l and m are next-nearest neighbours and the sender is in the middle, again quantum information storage can be achieved;

2.) if the sites l and m are more distant each other, entanglement waves propagate almost lossless in the region between the two defects and interference phenomena occur, like in a finite spin chain with open boundary.

If, instead, the singlet state is realized initially between one of the defects and the external spin, the concurrence with the external spin bounces between the two impurities, while the rest of the chain is not involved in the entanglement transmission. This effect can be explained by taking the defects strength equal and sufficiently high, so that the discrete states are highly localized around both impurity sites. Therefore the excitation can be transmitted only over these discrete states, again because the continuous energy band cannot receive the too high energy excitation. Looking at the expression of the two localized states, they turn out to be a coherent superposition of one-excitation state l and m , resulting in the two (orthonormal) maximally entangled states of the one-excitation Hilbert sector. The entanglement dynamics reduces also to a dynamics of a two-level system (the two levels being the localized states) where entanglement bounces with a Rabi frequency given by the energy difference of the two discrete eigenstates. As this energy difference tends to zero by increasing the distance between the impurities, the related entanglement transfer requires an increasing time interval (sec.3.3).

In conclusion, we have dealt with defected 1D spin systems from an quantum-information point of view. We examined the implications of the Anderson localization effect on the ground state entanglement content and quantum-state transmission's related problems. We have found several interesting phenomena, which permits, by minimal control operations, both quantum information storage and entanglement dynamics manipulation as well as entanglement generation.

Chapter 1

Entanglement

In this chapter we review some milestones in quantum physics, from the EPR paradox to Bell's inequalities, leading to the emerging of the entanglement's concept, sec.1.1. In sec.1.2, density operator formalism is introduced together with the main object of interest in quantum information theory (QIT): the qubit. In sec.1.3 some of the entanglement measures for bipartite systems are presented and in sec.1.4 we focus on some aspects of open system quantum theory, which will have application in the forthcoming work. The last section is devoted to a brief description of some common entanglement's applications. For general topics on the subject of this chapter see [1, 2, 3] and references therein.

1.1 Introduction to Entanglement

The first encounter with entanglement dates back to 1935, when Einstein, Podolsky and Rosen (EPR) published one of the most cited physics paper [4]. They supposed that quantum theory was not a complete theory, stating the condition of completeness as

Every element of physical reality must have a counterpart in the physical theory.

and defining the cited "element of reality" as the observable obeying the following

if, without in any way disturbing a system, we can predict with certainty...the value of a physical quantity, then there exist an

element of physical reality corresponding to this physical quantity.

They considered a two-particle system in an eigenstate of their relative position and total momentum, $|\Psi(1, 2)\rangle = |x_1 - x_2; p_1 + p_2\rangle$, which, according to quantum theory can exist as the two observables commute. Performing a Gedankenexperiment in which measuring x_1 one obtains x_2 , the latter must be an element of physical reality according to EPR; and the same argument applies to the determination of p_2 after a measure of p_1 is performed. As a result, the observed values x_2 and p_2 must exist, they argued, also before the measurement process as special relativity doesn't account for super-luminal actions. But $[x_2, p_2] \neq 0$ and quantum theory doesn't attribute any definite value to two non-commuting observables at the same time.

The EPR article was followed by an intense debate between two school's of thought, one, headed by Bohr, defending quantum theory, the other underlining its incompatibility with the axioms of local realism and proposing reconcilable alternatives, such as the hidden variable model.

After Bohm's work, the paradox became an algebraic contradiction submitted to experimental verification. Consider a two spin- $\frac{1}{2}$ particle state

$$|\Psi(1, 2)\rangle = \frac{1}{2} (|01\rangle - |10\rangle) \quad (1.1)$$

resulting, for example, from a decay of spin 0 particle. Looking at their x and y spin component we have that $s_x^{(1)} = -s_x^{(2)}$ and $s_y^{(1)} = -s_y^{(2)}$. So if quantum theory satisfies the axioms of local realism $s_x^{(1)} s_y^{(2)} = s_y^{(1)} s_x^{(2)}$, but quantum theory predicts $(s_x^{(1)} s_y^{(2)} + s_y^{(1)} s_x^{(2)}) |\Psi(1, 2)\rangle = 0$, so that the two observables are anti-correlated, $s_x^1 s_y^2 = -s_y^1 s_x^2$.

The algebraic contradiction was put in an experimentally verifiable form by Bell [5], who showed that there exists an upper limit for the correlations of space-like distant events if the principle of local realism has to be satisfied.

There exist different kinds of Bell inequalities depending on what system one considers, but always there are quantum states which violate the inequalities. Here we consider the inequality arising from measuring dichotomic variables on system A and B, the CHSH inequality[6].

On system A one measures observables Q and R , on system B, observables S and T , and each of them can assume only values ± 1 . So if the mean values of measurements are classically correlated then

$$\langle QS \rangle + \langle RS \rangle + \langle RT \rangle - \langle QT \rangle \leq 2 \quad (1.2)$$

But if we consider the singlet state given by eq.1.1 and choose the following set of observable: $Q = \sigma_z^A$, $R = \sigma_x^A$ and $S = \frac{-\sigma_z^B - \sigma_x^B}{\sqrt{2}}$, $T = \frac{\sigma_z^B - \sigma_x^B}{\sqrt{2}}$, then on the left side of eq.1.2 one obtains $2\sqrt{2}$. This results indicates that the singlet state contains non-local quantum correlations. Moreover in the Hilbert space of two qubits, the maximal violation of eq.1.2 is realized by the so called Bell states

$$|\Psi^\pm\rangle = \frac{1}{\sqrt{2}}(|01\rangle \pm |10\rangle) \quad |\Phi^\pm\rangle = \frac{1}{\sqrt{2}}(|00\rangle \pm |11\rangle) \quad (1.3)$$

Having defined so far entanglement as non-local quantum correlations between parties of a composite system, we have to account for more general states in which quantum systems can be found. In fact, generally the parties of a system, even if they are initially pure states, evolve in mixed states. This is because their evolution is not unitary, although the total system evolution is governed by an unitary operator. Moreover, it is quite common to have access to only a finite number of parties of the total system, so that one has to take somehow into account the interaction with the unobserved parties. This is equivalent to consider a statistical mixture of the parties we observe, with weights depending on the interaction. Therefore we have to introduce a formalism which is appropriate for dealing with mixed states: the density operator.

1.2 Density Operator

Density operators arise in quantum theory as soon as we want to describe no longer a single quantum object, but two or more. It is possible to arrive at its properties in two different ways: following the state vector formalism of quantum mechanics for the composite system and then looking at only one party or starting from more general principles.

Let's explore the first case relative to a bipartite system, but generalizations are straightforward. A general pure¹ state of the total system can be expressed as a vector $|\Psi\rangle_{AB} = \sum_{ij} a_{ij} |i\rangle_A |j\rangle_B$ in the Hilbert space having $\{|i\rangle_A \otimes |j\rangle_B\}$ as an orthonormal basis. If we look at the expectation value of a variable acting on A alone, $M_{AB} = M_A \otimes 1_B$, using the state vector formalism, we can write

¹this assumption is necessary as mixed states cannot be expressed by a vector

$$\langle M \rangle = \langle \Psi | M | \Psi \rangle = \text{Tr}(\rho_A M_A)$$

In the last equality $\rho_A = \sum_{ijk} a_{ij} a_{jk}^* |i\rangle_A \langle j|_A \equiv \text{Tr}_B(|\Psi\rangle \langle \Psi|)$ is the density operator of party A, obtained by tracing the total density operator over the states of party B. We will postpone the discussion of the formal properties of density operators in the following, where an axiomatic approach will be given; let's just say now that the state of party A cannot be expressed by a state vector, because in general it's density operator, in the basis in which it has a diagonal matrix representation, is given by

$$\rho_A = \sum_i p_i |\phi_i\rangle \langle \phi_i| \quad (1.4)$$

with $0 < p_i \leq 1$ and $\sum_i p_i = 1$. So ρ_A is not a projector on a one-dimensional space, unless only one of the p_i is different from zero. It follows that ρ_A describes a pure state (and in that case state vector formalism is applicable) only if $\text{Tr}(\rho_A^2) = 1$; if, on the other hand, $\text{Tr}(\rho_A^2) < 1$ then, from eq.1.4, one says that system A is composed by an incoherent superposition of states $|\phi\rangle_A$; that is, ρ_A describes an ensemble of pure quantum states each occurring with probability p_i .

In this framework we can see also the role of entanglement in the decoherence process. Let's assume we have access to a system A interacting with an environment, system B. This interaction entangles the states of our system A with the states of the environment; the latter however is constituted by a huge number of degrees of freedom. Therefore, being in the impossibility to monitor the environment, system A evolves in a state described by eq.1.4: a statistical mixture.

The axiomatic way leading to density operator formalism starts with Gleason's theorem. A quantum state has to be an object on which measurement can be defined consistently. Considering a set of orthogonal measures, described by projectors E_i , a quantum state p is a map that fulfills the following conditions:

- $0 \leq p(E) \leq 1$, with $p(0) = 0$ and $p(1) = 1$, meaning that if we make no measure on state p we obtain 0, if we make all 1;
- if $E_i E_j = 0$ then $p(E_i + E_j) = p(E_i) + p(E_j)$, meaning that, as orthogonal projections are mutually exclusive, the probabilities assigned to their outcomes must be additive

Gleason's theorem states that for Hilbert spaces with $d \geq 2$, every mapping satisfies $p(E) = \text{Tr}(\rho E)$, where ρ is the density operator. The cornerstone in the demonstration is the second requirement and it's also the reason of the lower bound on the dimensionality of Hilbert space, because in $d = 2$ there is only one projector satisfying this requirement and consequently there are many different maps.

So density matrix formalism turns out to be the most general possible, and every other description reduces to it. In order to be a density operator, ρ needs to fulfill two conditions:

1. (unit trace) $\text{Tr}(\rho) = 1$
2. (positivity) $\forall |\varphi\rangle \in \mathcal{H}, \langle \varphi | \rho | \varphi \rangle \geq 0$

The first condition is equivalent to a completeness relation, the second implies that the density operator is hermitian. So to any isolated physical system there is associated a density operator acting on the Hilbert space \mathcal{H} spanned by the eigenvectors of the density operator spectral decomposition; the evolution of a closed system ρ is described by unitary operators

$$\rho(t_2) = U(t_2, t_1)\rho(t_1)U^\dagger(t_2, t_1)$$

and measurements are described by hermitian operators M_m , where the capital letter is the observable being measured and the lower case is the outcome. So mean values are obtained by $\langle M \rangle = \text{Tr}(\rho M)$, the probability of the outcome m is $p(m) = \text{Tr}(M_m^\dagger M_m \rho)$ and the state of the system immediately after the measurement is $\rho = \frac{M_m^\dagger M_m \rho}{\text{Tr}(M_m^\dagger M_m \rho)}$.

1.2.1 Reduced Density Operator

Let's consider a system S composed of many different parties and we act a bipartition on it: $S = A + B$. The complete system is described by ρ_{AB} , but we are interested (or we have access) only at one of them, say A. Therefore we have to perform a partial trace operation (PT) on the total density operator ρ_{AB} to obtain the reduced density operator describing the subsystem A:

$$\rho_A = \sum_i \langle i | \rho_{AB} | i \rangle \doteq \text{Tr}_B(\rho_{AB})$$

where $\{|i\rangle\}$ is any orthonormal (O.N.) basis of party B . The reason for this choice resides in the observation that PT is the unique operation that satisfies the measurements requirement of observable quantities of subsystems. It turns out that PT gives some insights into the nature of entangled states. If we consider one of the pure Bell states and perform a PT, the reduced density operator of both parties is $\frac{1}{2}\mathbf{1}$, which is not a pure state, moreover it is a completely mixed state.

An important property of density operator that will be used in the definition of entanglement's measures is that they form a convex subset of the $N \times N$ hermitian matrix vector space as can be seen from eq.1.4, with pure states on the boundary. So any point in the interior of the convex subset, that is every mixed density matrix, can be expressed as a convex sum of pure states.

1.2.2 Schmidt Decomposition

A useful expression for entanglement definitions of a bipartite pure state is given by the Schmidt decomposition. A general pure state in $\mathcal{H}_A \otimes \mathcal{H}_B$ is given by $|\Psi\rangle_{AB} = \sum_{ij} a_{ij} |i\rangle_A |j\rangle_B$, which, in turns, can be written as

$$|\Psi\rangle_{AB} = \sum_i \sqrt{p_i} |i\rangle_A |i'\rangle_B \quad (1.5)$$

where $|i\rangle_A$ and $|i'\rangle_B$ are O.N. basis of H_A and H_B respectively. Eq.1.5 is the Schmidt decomposition of the given pure state, and, in general, it isn't possible to use the same O.N. basis to expand a different pure state $|\Phi\rangle$ belonging to H_{AB} because $|i'\rangle = p^{-\frac{1}{2}} \sum_j a_{ij} |j\rangle$ so that the basis used in eq.1.5 depends upon the pure state being expanded. Schmidt decomposition reveals it's utility in computing reduced density operators ρ_A and ρ_B , which will be $\rho_A = \sum_k p_k |k\rangle\langle k|$ and $\rho_B = \sum_k p_k |k'\rangle\langle k'|$. Both operators have the same non zero eigenvalues and the number of them is the Schmidt number. If this number is greater than one then the parties A and B are entangled, otherwise they aren't. This can be understood considering that in eq.1.5 a Schmidt number equal to one means that $|\Psi\rangle_{AB} = |i\rangle_A |i'\rangle_B$, so the pure state is separable. Unfortunately there exist pure states of a n -partite system, with $n > 2$, that don't admit a Schmidt decomposition, so this is a tool only for revealing entanglement in bipartite systems.

The systems with which quantum information theory (QIT) generally

deals with are two-level systems: these are consistently described attributing them a fictitious $\frac{1}{2}$ spin, and in QIT one refers to them with the term qubit.

1.2.3 The Qubit

A qubit is the quantum analogue of the classical bit. As the classical bit it can assume two values, say 0 and 1, when measured along some axis ² but, here's quantum, it can be also in a superposition of the two states:

$$|qubit\rangle = a|0\rangle + b|1\rangle \equiv \cos\frac{\theta}{2}|0\rangle + e^{i\phi}\sin\frac{\theta}{2}|1\rangle \quad (1.6)$$

A qubit belongs to the 2-dimensional Hilbert space \mathcal{H}^2 and all operations on it, due to norm preservation, can be represented by 2x2 unitary matrices. An irreducible representation of this group is given by the identity and the Pauli matrices

$$\sigma_0 = \begin{pmatrix} 1 & 0 \\ 0 & 1 \end{pmatrix} \quad \sigma_x = \begin{pmatrix} 0 & 1 \\ 1 & 0 \end{pmatrix} \quad \sigma_y = \begin{pmatrix} 0 & -i \\ i & 0 \end{pmatrix} \quad \sigma_z = \begin{pmatrix} 1 & 0 \\ 0 & -1 \end{pmatrix} \quad (1.7)$$

A useful picture of single qubit density matrices, and of the operations on them, is the Bloch ball, fig.1.1. For a single qubit the density matrix is a 2×2 hermitian matrix having three independent parameters, thus the most general $\rho^{(1)}$ can be expanded in the $\{1, \sigma_x, \sigma_y, \sigma_z\}$ basis:

$$\rho^{(1)} = \frac{1}{2} \sum_{\alpha=0}^3 q^\alpha \sigma_\alpha \quad (1.8)$$

where q^α are the cartesian components of a vector related to the mean values of the Pauli matrices: $q^\alpha = \langle \sigma_\alpha \rangle$. The condition of positivity implies that $|q|^2 \leq 1$, so to every point of the Bloch ball corresponds univocally a single-qubit density matrix. Only the points on the boundary of the ball, that is on the enveloping surface of the convex subset are pure states; on the contrary the origin is a completely mixed state $\rho = \frac{1}{2}1$; the boundary to the origin the state becomes more and more mixed.

²From now on we choose z as the quantization axis, and qubits measured in the σ_z eigenstates basis are said to be expressed in the computational basis. Moreover we adopt the conventions $|\uparrow\rangle = |0\rangle = \begin{pmatrix} 1 \\ 0 \end{pmatrix}$ and $|\downarrow\rangle = |1\rangle = \begin{pmatrix} 0 \\ 1 \end{pmatrix}$.

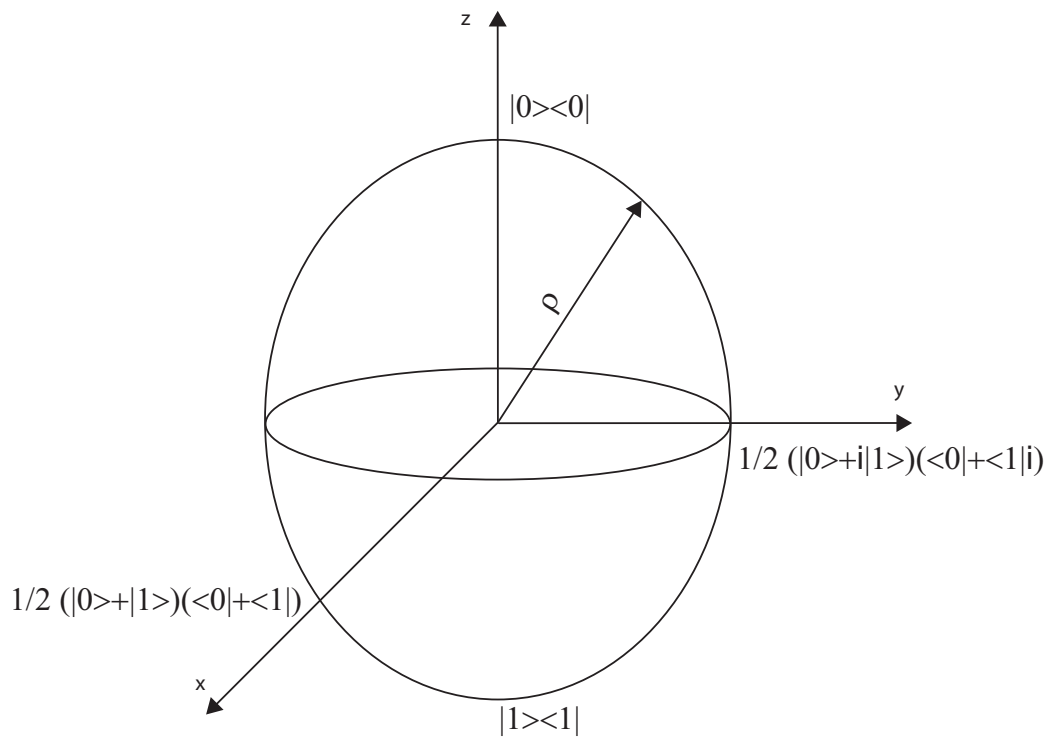


Figure 1.1: Bloch ball with some pure state density matrices in the σ_z basis.

Two qubits density matrices belong to \mathcal{H}^4 , and their operator expansion representation in terms of Pauli matrices is

$$\rho^{(2)} = \frac{1}{4} \sum_{\alpha, \beta=0}^3 q^{\alpha\beta} \sigma_\alpha \otimes \sigma_\beta \quad (1.9)$$

where the 15 independent coefficients accounts for both single spin properties and the correlations between spins: $q^{\alpha\beta} = \langle \sigma_\alpha \sigma_\beta \rangle$.

1.3 Entanglement Measures

In the previous sections we have described entanglement as the quantum correlations that can reside in multipartite systems. Now we trace a more precise and general distinction between classical and quantum correlation than that due to Bell's inequality. We define classical correlations those which can be generated, between parties of a multipartite system, by performing a class of operations that includes local quantum operations (on each party) and classical communication (between parties), in brief LOCC. On the other hand, quantum correlations, that is entanglement, are those which can't be generated by LOCC operations. It is possible also to re-state the latter sentence in a stronger way: LOCC operations cannot increase the amount of entanglement shared by the parties of a system³. As a corollary we obtain that entanglement does not change under local unitary operations. In fact, as local unitary operations can be inverted by local unitary operations, the two states are related by a LOCC operation, therefore they must have the same amount of entanglement.

By only a LOCC-based definition of entanglement descends that separable states contain no entanglement, as they can be generated by use of LOCC operations alone. On the contrary, all non-separable states are entangled.

Henceforth we focus only on entanglement between parties of a bipartite system, for which a more exhaustive theory has been developed and because in our work we have to deal only with bipartite entanglement. The first step in order to define an entanglement measure is to realize whether there exist states which are more entangled than others, and if there exists an upper bound (the lower being zero) on the value entanglement takes. In the

³This monotony constraint allows the use of the term entanglement monotone for each proposed entanglement measure satisfying the LOCC constraint.

following the entanglement measures are divided into those referring to pure states and those referring to mixed states.

In two-party systems composed of two fixed d -dimensional sub-systems, referred to as qudits, it is possible to identify maximally entangled pure states, given by

$$|\Phi_d^+\rangle = \frac{1}{\sqrt{d}} (|00\rangle + |11\rangle + \dots + |d-1 d-1\rangle)$$

and local-unitarily equivalent states. If the bipartite system is composed of qubits, the maximally entangled states become the Bell states, as previously reported⁴.

If the system is in a pure state, it has been proved that there exists a unique measure of the entanglement shared among the parties: namely the entropy of entanglement [7] or the von Neumann entropy

$$E(\rho_A) \equiv S(\rho_A) = -\text{Tr}(\rho_A \log_2 \rho_A) \quad (1.10)$$

Due to Schmidt decomposition, the same amount results for $E(\rho_B)$.

1.3.1 Entropy

Entropy had a central relevance long before quantum information theory; it enters already in classical information theory after the work of Shannon, who was concerned with the question: What is the rate of redundancy of a message?

Answering this will be useful for compressing the original message and the result is the noiseless coding theorem. It states that a message, i.e. a string of n letters chosen from k letters $\{x_k\}$ each occurring with probability $p(x_k)$, can be compressed to a message composed of $nH(X)$ bits. The quantity $H(X)$ is known as Shannon entropy of the ensemble $X = \{x, p(x)\}$, eq.1.11 can be also seen as the average amount of information that a letter x chosen from the ensemble carries.

$$H(X) = -\sum_k p(x_k) \log_2 p(x_k) \quad (1.11)$$

⁴The non-existence of a similar statement in multipartite systems is one of the difficulties of a related entanglement measure theory.

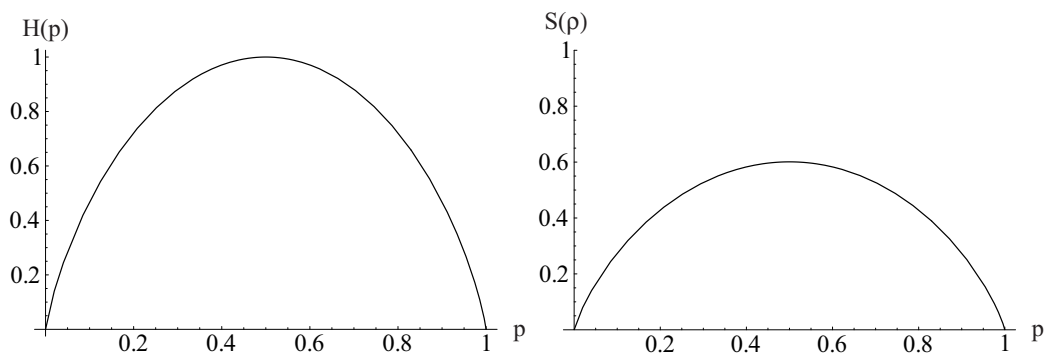


Figure 1.2: left: Binary entropy (eq.1.12) of a two-outcome random variable; right: von Neumann entropy (eq.1.10) for $\rho = p|0\rangle\langle 0| + \frac{1-p}{2}(|0\rangle + |1\rangle)(\langle 0| + \langle 1|)$. As quantum information can be encoded also in non-orthogonal states the amount of information it carries is different from the classical case where information is carried by, in principle, distinguishable letters.

If we consider an ensemble made of only two letters, denoted by 0 and 1, then Shannon entropy is given the name of binary entropy (fig.1.2).

$$H(p) = -(p \log_2 p + (1 - p) \log_2(1 - p)) \quad (1.12)$$

Now let's turn to QIT, assuming that the letters are quantum states characterized by a density matrix ρ_x occurring with probability p_x . So Shannon entropy becomes von Neumann entropy⁵ given by eq.1.10

This quantity reduces to eq.1.11 if the ensemble is made of orthogonal (commuting) density matrices; if, on the other hand, the ρ_x 's in $\rho = \sum p_x \rho_x$ don't commute among each other, there arise substantial differences (fig.1.2).

So if we consider maximally entangled pure bipartite systems, like the Bell states, we have $S(\rho_A) = S(\rho_B) = 1$, on the other hand $S(\rho_{AB}) = 0$, meaning that even if the joint system is completely known, the state of each party is completely unknown.

⁵In eq.1.10 logarithms can be also taken in base d , with d given by the dimensionality of the parties, in order to normalize entanglement; but if we consider the amount of entanglement in a Bell state, and refer to it with the term ebit, then ebits can be considered as a unit of measure of entanglement. So if the bipartite system is composed of parties A and B, the quantity $S(\rho_A) = -Tr(\rho_A \log_2 \rho_A)$ represents the number ebits they share.

Von Neumann entropy is a natural entanglement measure as it fulfills the subsequent requirement:

1. entanglement is an extensive property, so that if two systems are independent $E(AB) = E(A) + E(B)$;
2. entanglement is conserved under local unitary operations U , so that $E(A) = E(UA)$;
3. entanglement cannot increase (but can decrease) under local non-unitary operations, e.g. a measurement;
4. entanglement can be concentrated and diluted with unit asymptotic efficiency by means of local actions and one-way classical communication [8].

In QIT a few other entropy definitions can be quite useful

- quantum relative entropy $S(\rho_A||\rho_B) \equiv Tr(\rho_A \log \rho_A) - Tr(\rho_A \log \rho_B)$, for which the Klein's inequality holds $S(\rho_A||\rho_B) \geq 0$, with equality iff $\rho_A = \rho_B$;
- quantum conditional entropy $S(\rho_A|\rho_B) \equiv S(\rho_{AB}) - S(\rho_B)$, which is a measure of our ignorance about system A once we know B;
- quantum mutual information $S(\rho_A : \rho_B) \equiv S(\rho_B) - S(\rho_B|\rho_A)$ which is a measure of the information about system A shared by system B.

Also in classical information theory one can define similar entropy measures (fig.1.3), where the role of von Neumann entropy is played by Shannon entropy; but some properties, valid in CIT fails in QIT, due to entanglement. Let's consider the conditional entropy, which in CIT obeys $H(A|B) \geq 0$, i.e. $H(A, B) \geq H(A)$, with the intuitive meaning that the ignorance about the composite state A+B cannot be less than the ignorance upon state A alone. In QIT this is no longer true, for entangled parties of a pure bipartite state $S(\rho_A|\rho_B) < 0$, as can be easily checked for Bell states.

A list of mathematical properties of von Neumann entropy is given, with the remark that they are valid also for the entanglement measure of pure states:

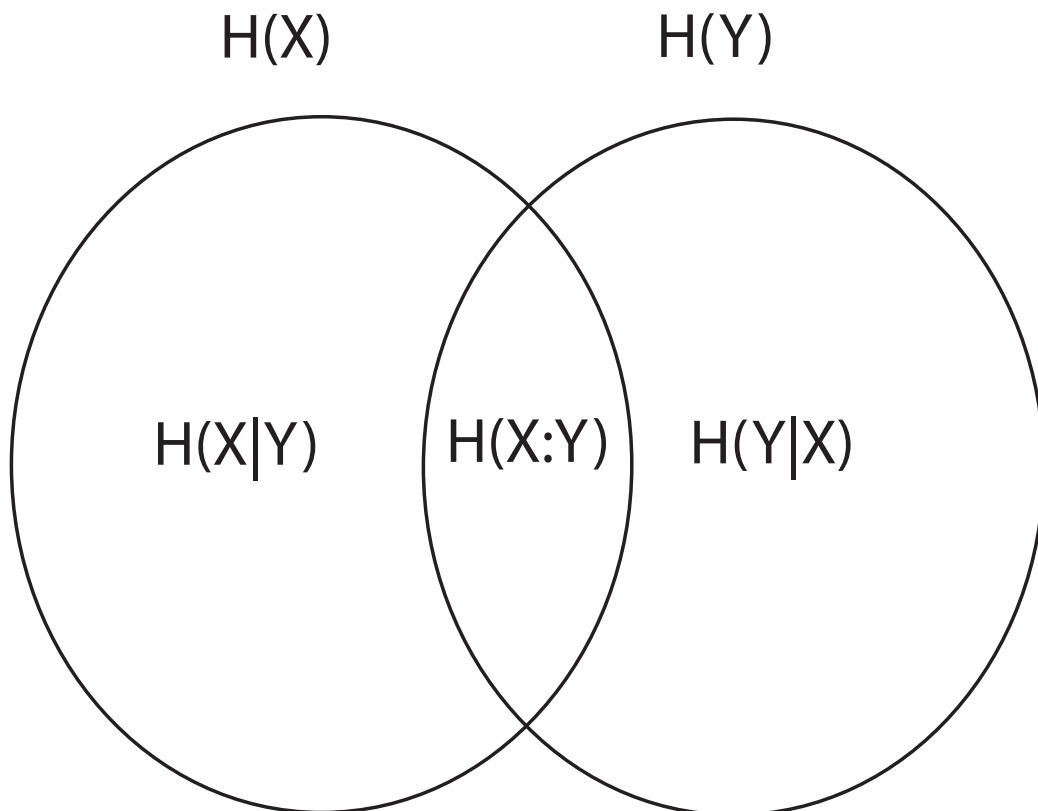


Figure 1.3: Relationships between various entropies: the Shannon entropy $H(X)$, the conditional entropy $H(X|Y)$, and the mutual entropy $H(X : Y)$.

non-negativity $\log D \geq S(\rho) \geq 0$ with equality on the left (right) iff ρ describes a completely mixed (pure) state, because there's total (no) lack of knowledge in a system described by a state vector;

invariance entropy is invariant under unitary change of basis $S(U\rho U^{-1}) = S(\rho)$, since eigenvalues are also invariant under the transformation.

concavity $S(\sum p_i \rho_i) \geq \sum p_i S(\rho_i)$, where $p_i \geq 0$ and $\sum p_i = 1$, this arises from the convexity of the logarithmic function and means that our knowledge is greater if we have information about the preparation of the quantum state

entropy of measurement ⁶ $S(\rho') \geq S(\rho)$, where ρ' and ρ describe the system respectively after and before a projective measurement⁷, with equality holding iff $\rho' = \rho$. On the other hand, generalized measurements⁸ can decrease entropy.

subadditivity $S(\rho_{AB}) \leq S(\rho_A) + S(\rho_B)$ with equality iff $\rho_{AB} = \rho_A \otimes \rho_B$. This accounts for the presence of correlations⁹ between the two parties.

strong subadditivity $S(\rho_{ABC}) + S(\rho_B) \leq S(\rho_{AB}) + S(\rho_{BC})$, where ρ_i describes the parties of a tripartite system. A lot of interesting entropy's properties can be derived from this inequality. One of them, for example, is $S(\rho_A) + S(\rho_B) \leq S(\rho_{AC}) + S(\rho_{BC})$, which is responsible for the fact that even if $S(\rho_A) \geq S(\rho_{AC})$ and $S(\rho_B) \geq S(\rho_{BC})$ are both possible, strong subadditivity negates this possibility to hold simultaneously.

1.3.2 Mixed-State Entanglement

The necessity of a measure of the amount of entanglement in a mixed state comes from the aim to quantify entanglement also in the case where the two parties are not component of a pure state. This is quite common as

⁶this holds only in the case we don't acquire the result of the measure

⁷projective measurements are a special class of quantum measurement represented by operators M_m for which holds, apart the usual completeness relation $\sum_m M_m^\dagger M_m = 1$, also the condition that they're orthogonal projectors, that is $M_m M_{m'} = \delta_{mm'} M_m$

⁸generalized measurements are represented by operators which are not projectors

⁹Nevertheless it isn't a signature of non-local quantum correlations as the same property holds for Shannon entropy

generally systems A and B are part of a bigger system which comprehends the environment, and dynamical evolution of system A+B and E transforms the possible initial pure state of A and B in a mixed one.

For parties of a mixed state a unique measure for entanglement doesn't exist; also the semi-quantitative Bell's criterion fails as there are states which don't violate any Bell inequality and nevertheless exhibit non-local behaviour [9].

In relation to a general mixed state ρ_{AB} three entanglement measures can be defined:

1. entanglement of formation, E_F , which gives the (asymptotic) number of Bell states needed in order to generate ρ_{AB} ;
2. entanglement of distillation with two-way communication, D_2 , giving the (asymptotic) number of Bell states that can be extracted from ρ_{AB} with the help of classical communication between the parties;
3. entanglement of distillation with one-way communication, D_1 , which gives the (asymptotic) number of Bell states that can be extracted from ρ_{AB} with the help of classical communication only from one party to another.

It can be shown that $E_F \geq D_2 \geq D_1$, with equality holding only for pure states.

Entanglement of Formation

The definition of this measure requires the following iter:

1. the entanglement of formation of a bipartite pure state $|\Psi\rangle$ is the von Neumann entropy of either the reduced density operators;
2. the entanglement of formation of an ensemble of bipartite pure states $E = \{p_i, |\Psi\rangle\}$ is the ensemble average of the entanglement of formation of the pure states of the ensembles;
3. the entanglement of formation of a bipartite mixed state is the minimum of the above defined entanglement averages over all possible pure states decomposition of the mixed state.

Let's illustrate with an example how does it work. The first point is simply a redefinition of von Neumann entropy as entanglement of formation; for the second and third point we consider a totally mixed bipartite system, $\rho = \frac{1}{4}\mathbb{1}$. Among all possible decomposition of ρ we need for our purpose only two:

- $\rho' = \frac{1}{4}(|00\rangle\langle 00| + |01\rangle\langle 01| + |10\rangle\langle 10| + |11\rangle\langle 11|)$
- $\rho'' = \frac{1}{4}(|\Psi^-\rangle\langle \Psi^-| + |\Psi^+\rangle\langle \Psi^+| + |\Phi^-\rangle\langle \Phi^-| + |\Phi^+\rangle\langle \Phi^+|)$

The entanglement of formation of the first ensemble is identically zero, for the second it is 1. Finally the third definition tells us that the mixed state ρ has entanglement 0. So the complete expression for the entanglement shared between parties of a mixed bipartite quantum system is given by

$$E_F(\rho) = \inf_{(p_k, |\Psi_k\rangle)} \left[\sum_k p_k E(|\Psi_k\rangle\langle \Psi_k|) \right] \quad (1.13)$$

This measure involves a minimization procedure that can be not at all simple to handle, but, if the two parties are two-level systems, Wootters [10] has related the entanglement of formation to a quantity, the concurrence C , which is easier to calculate. As E_F relies on entanglement of pure states, there's a need for the relationship between entanglement of pure state, i.e. as measured by von Neumann entropy, and concurrence: $E(|\Psi\rangle) = \mathcal{E}(C(|\Psi\rangle))$, where $\mathcal{E}(C) = h\left(\frac{1+\sqrt{1-C^2}}{2}\right)$ and $h(x) = -x \log_2 x - (1-x) \log_2(1-x)$, i.e. the binary entropy of x . The function \mathcal{E} is monotonically increasing from 0 to 1 as C goes from 0 to 1, so concurrence can be taken as a measure of entanglement itself. The concurrence is defined in terms of the spin flip transformation, which for a pure state of a single qubit gives the spin flipped state $|\tilde{\Psi}\rangle = \sigma_y |\Psi^*\rangle$, corresponding to the time reversal transformation. For the general state ρ of two qubits, the corresponding spin-flipped state is $\tilde{\rho} = (\sigma_y \otimes \sigma_y) \rho^* (\sigma_y \otimes \sigma_y)$. Finally the concurrence of a pure state of two qubits is defined as $C(\Psi) = |\langle \Psi | \tilde{\Psi} \rangle|$. If we refer instead to mixed states described by the density matrix ρ , always in the computational basis, also concurrence is given by $C(\rho) = \max[0, \lambda_1 - \lambda_2 - \lambda_3 - \lambda_4]$, where λ_i are the square root of the eigenvalues, in decreasing order, of the non-hermitian matrix $R = \rho \tilde{\rho}$ or, equivalently, the eigenvalues of the hermitian matrix $R' = \sqrt{\sqrt{\rho} \tilde{\rho} \sqrt{\rho}}$.

Concurrence results a powerful tool in evaluating the entanglement between two qubits¹⁰ in a mixed state, but it can be possible, that entanglement is shared between more than two parties [12]. Without entering the multipartite entanglement properties, we introduce only the concept of tangle. Considering a pure state system composed of n qubits, partitioned so that party A results composed of $(n - 1)$ qubits and party B only from the i -th qubit, then the total amount of entanglement between the two parties is given as usual by the von Neumann entropy $E(\rho^{(1)}) = -Tr(\rho^{(1)} \log_2 \rho^{(1)})$, where $\rho^{(1)}$ is the one-site density matrix of the partition B. One defines the one-tangle [13] as $\tau^1(\rho^{(1)}) = 4 \det(\rho^{(1)})$ and its relation to von Neumann's entropy is exactly the same as for concurrence. In the tangle-measure of entanglement between the qubit i and the $(n - 1)$ qubit are contained all forms of possible entanglement, the pairwise one, as measured by concurrence, as well as the multipartite one, moreover it is an additive quantity. So the following CKW inequality arises: $\sum_{j \neq i} C_{ij}^2 \leq \tau_i^{(1)}$. It's meaning is that on the left side is reported the pairwise entanglement between qubit i and each of the remaining qubits, on the right its total amount of entanglement.

Entanglement of Distillation

For this entanglement measure an expression like eq.1.13 isn't known, but upper and lower bound are obtainable. The upper bound is given just by E_F , because it is a non-increasing quantity under LOCC; lower bound depends on the entanglement purification protocol (EPP) chosen.

1.4 Quantum Operations

As seen previously, entanglement measures rely on the density operator formalism; also it is useful to introduce a class of operations, $\{\mathcal{E}\}$, acting on the density operator vector space such that $\mathcal{E} : \mathcal{E}(\rho) = \rho'$ describes a stochastic evolution of the quantum system. Following an axiomatic approach we require the map \mathcal{E} to fulfill the following requirements:

1. $0 \leq Tr(\mathcal{E}(\rho)) \leq 1$, defining $Tr(\mathcal{E}(\rho))$ as the probability that the process represented by \mathcal{E} takes place.

¹⁰if the parties are not qubits but higher-dimensional systems concurrence has been generalized to I-concurrence [11]

2. $\mathcal{E}(\sum_i p_i \rho_i) = \sum_i p_i \mathcal{E}(\rho_i)$, that is, \mathcal{E} is a convex-linear map
3. \mathcal{E} is a completely positive map, meaning that if ρ_{AB} is a density operator of the joint system A+B, then also $\mathcal{E}(\rho_{AB})$ must be a density operator, where $\mathcal{E}(\rho_{AB}) = 1_A \otimes \mathcal{E}_B$. An example of a positive map, but not completely positive, is given by the transposition operation on a single qubit.

A theorem states that a map, in order to satisfy these requirements, must admit an operator-sum representation

$$\mathcal{E}(\rho) = \sum_k E_k \rho E_k^\dagger \quad (1.14)$$

where the set of operators E_k maps the input n-dimensional Hilbert space to the m-dimensional Hilbert space; and satisfy $\sum_{k=1}^{nm} E_k^\dagger E_k \leq 1$. If equality holds the map is said trace-preserving, as happens for trace and partial trace operations.

The outlined formalism is useful when dealing with open quantum systems: the evolution of the parties may not be unitary and it is described by the map

$$\mathcal{E}(\rho_A) = Tr_E (U (\rho_A \otimes \rho_E) U^\dagger) \quad (1.15)$$

where the assumption has been made that the bipartite system, composed of system A, which we generally access, and system E, the environment, forms a closed system and starts its evolution in a product state. This last assumption isn't generally true, because A and E interact also before we start to observe them and correlations are built up, but they can be washed out as soon as the experimentalist prepares the observed system in a definite state.

Eq.1.15 can be put in an operator-sum representation like eq.1.14 involving only operators acting on the Hilbert space of system A. Assuming that the environment starts in a pure¹¹ state, $|e_0\rangle$ belonging to the O.N. basis $\{|e_k\rangle\}$, then the operators elements of the map are $E_k = \langle e_k | U | e_0 \rangle$ acting on system A.

Following a system-environment interpretation of quantum operations formalism, we discuss the situation in which our system is composed from

¹¹also this assumption isn't generally true, but it is possible to introduce an auxiliary system purifying the environment into the desired pure state

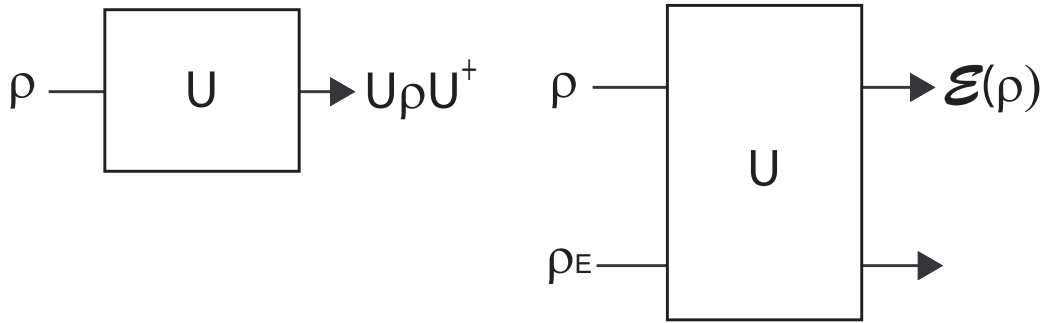


Figure 1.4: evolution of a closed system (left) an open system (right) left unobserved. The density matrix describing the total system (left) evolves by means of unitary operators, whereas the evolution of a party of the total system (right) exhibits a non-unitary evolution.

one qubit undergoing some kind of trace-preserving quantum operation due to his coupling to the environment, which acts like a quantum channel.

Depolarizing Channel

In this case the environment acts on the qubit causing an evolution to a completely mixed state: $\mathcal{E}(\rho) = \frac{1}{2}\mathbf{1}$. The operator sum representation is given by the set $\{\sqrt{1-p}\mathbf{1}, \sqrt{\frac{p}{3}}\sigma_x, \sqrt{\frac{p}{3}}\sigma_y, \sqrt{\frac{p}{3}}\sigma_z\}$ where p is the probability that one of the possible one-qubit operations took place;

Phase Damping Channel

In this case environment causes the evolution of the qubit in a statistical mixture of states, i.e. it induces the decay of the off-diagonal terms of ρ in the so-called pointer basis¹² $\{|i\rangle\}$: $\mathcal{E}(\rho) = \sum_i p_i |i\rangle\langle i|$. Its operator sum representation is given by

$$\left\{ \sqrt{1-p}\mathbf{1}, \sqrt{p} \begin{pmatrix} 1 & 0 \\ 0 & 0 \end{pmatrix}, \sqrt{p} \begin{pmatrix} 0 & 0 \\ 0 & 1 \end{pmatrix} \right\}$$

¹²the basis that diagonalizes the observable(s) of the qubit involved in the system-environment interaction

Amplitude Damping Channel

In this case the environment causes the spin to relax in his ground state $|1\rangle$, after $t \rightarrow \infty$, via an energy dissipation process: $\mathcal{E}(\rho) = |1\rangle\langle 1|$. The connected representation is

$$\left\{ \begin{pmatrix} 1 & 0 \\ 0 & \sqrt{1-p} \end{pmatrix}, \begin{pmatrix} 0 & \sqrt{p} \\ 0 & 0 \end{pmatrix} \right\}$$

As we will see in the next chapter the spin chain driven by the XX interactions acts like an amplitude damping channel, but the introduction of a defect can significantly reduce this effect.

1.4.1 Fidelity

One of the most import tasks in order to realize quantum information based devices is the transfer of a quantum state in the space-time domain with an high degree of similarity between the input and the output states. So the necessity arises of the definition of a measure reporting how much two quantum states, $\rho(t)$ and $\rho'(t')$, resemble each other. A natural approach to this measure is the usual concept of distance, between quantum states in the Hilbert space. For finite-dimensional systems one can define the trace distance

$$D(\rho(t), \rho'(t')) \equiv \frac{1}{2} \|\rho - \rho'\| \quad (1.16)$$

where $\|\cdot\|$ denotes the trace norm

$$\|A\| \equiv Tr(\sqrt{A^\dagger A})$$

where the positive value of the square root has to be taken.

Applying the definition to two qubits described by eq.1.8 one obtains $D(\rho, \rho') = \frac{1}{2} |\sum_\alpha (q^\alpha - q'^\alpha)|$, i.e. half the euclidean distance of the Bloch vectors. Some important theorems of trace-distance eq.1.16 are:

- $D(\rho, \rho') = D(U\rho U^\dagger, U\rho' U^\dagger)$, $\forall U$ unitary. It can be understood thinking at unitary operators as a rotation of the Bloch ball.
- $D(\mathcal{E}(\rho), \mathcal{E}(\rho')) \leq D(\rho, \rho')$ for all \mathcal{E} trace preserving quantum operations. An important case is given when the quantum operation \mathcal{E} is the partial

trace, $D(\mathcal{E}(\rho_A), \mathcal{E}(\rho'_A)) \leq D(\rho_{AB}, \rho'_{AB})$, meaning that distinguishing quantum states becomes harder having less information.

Trace distance defines a metric on density operator's Hilbert space, but in many applications it turns out to be simpler to relate the closeness of quantum state to another quantity, the fidelity.

$$F(\rho, \rho') \equiv \text{Tr} \left(\sqrt{\left(\sqrt{\rho'} \sqrt{\rho} \right)^\dagger \left(\sqrt{\rho'} \sqrt{\rho} \right)} \right) \quad (1.17)$$

Although fidelity isn't a metric, it has features similar to those of trace distance.

- $F(U\rho U^\dagger, U\rho' U^\dagger) = F(\rho, \rho')$, where U is an unitary operator;
- $F(\mathcal{E}(\rho), \mathcal{E}(\rho')) \geq F(\rho, \rho')$ for all \mathcal{E} trace preserving quantum operations. The inequality is reversed with respect to trace distance, because increasing fidelity means that the states are more similar.

If we look for the distance between a generic state ρ' and a pure one, $\rho = |\Psi\rangle\langle\Psi|$, eq.1.17 gives

$$F(\rho, \rho') = \langle\Psi|\rho'|\Psi\rangle \quad (1.18)$$

if also $\rho' = |\Phi\rangle\langle\Phi|$, $F(\rho, \rho') = |\langle\Psi|\Phi\rangle|^2$. The relation between the trace distance and the fidelity is given by

$$1 - F(\rho, \rho') \leq D(\rho, \rho') \leq \sqrt{1 - F(\rho, \rho')^2}$$

1.5 Application of Entanglement

As entanglement concept is a peculiar feature of quantum mechanics, it has widely-spread applications, both theoretical and technological ones. For the latter it's useful to stress that in any quantum communication experiment the aim of distributing quantum particles between different places is equivalent of distributing entanglement among the same places. In the sense that if we could transport a quantum state without any decoherence, then the amount of entanglement shared by the same state is perfectly distributed too. In the reverse sense, if the entanglement shared by quantum states could be

distributed perfectly, then, with a small amount of classical communication, we could use teleportation to achieve perfect quantum-state transfer.

The use of entanglement in technological applications relies in its use as a resource, in the sense that there are no other ways to achieve the same result, that is the generation of what has been defined as quantum correlations: entanglement cannot increase by LOCC alone (sec.1.3.1).

Entanglement as a theoretical tool in our world's investigation is motivated by the role quantum correlations play in a great variety of physical phenomena: from environment-induced decoherence, offering an explanation, although not exhaustive, of the emergence of the classical world, to many-particle quantum physics, where collective behaviour (e.g. quantum phase transitions) and particle correlations are strongly related.

In the following we review briefly some proposed entanglement applications, limiting our discussion only to scenarios involving pure states, but no generality is lost because of the possibility to perform purification protocols on mixed states in order to concentrate entanglement into pure states.

1.5.1 Dense Coding

Suppose Alice and Bob share one party of a maximally entangled state, say $|\Psi^-\rangle$, and Alice wants to send two bit of information by sending only one qubit. She can achieve this task[14] sending his member of the $|\Psi^-\rangle$ state. Effectively she can perform four types of operations on her party transforming the initial EPR state into another one

$$\mathbf{1}|\Psi^-\rangle = |\Psi^-\rangle \quad \sigma_x|\Psi^-\rangle = |\Phi^-\rangle \quad \sigma_y|\Psi^-\rangle = -|\Phi^+\rangle \quad \sigma_z|\Psi^-\rangle = -|\Psi^+\rangle$$

Then she sends the qubit in her possession to Bob who can perfectly distinguish between the four orthonormal Bell states, with an appropriate measure, which one he received. Recalling that 2 bit of classical information reside in a Bell state a dense coding protocol has been performed.

1.5.2 Teleportation

Suppose Alice and Bob share one party of a maximally entangled state, let's say $|\Psi^+\rangle$; but now Alice wants to send to Bob an unknown quantum state

$$|\varphi\rangle = \alpha|0\rangle + \beta|1\rangle \tag{1.19}$$

using only classical communication channels. Again she will be able to achieve this task using entanglement properties[15]. The initial state of the three qubits, Alice having only the first two, is

$$|\Upsilon\rangle = \frac{1}{\sqrt{2}} (\alpha|0\rangle (|01\rangle + |10\rangle) + \beta|1\rangle (|01\rangle + |10\rangle))$$

Applying a C-NOT gate on her qubits the state becomes

$$|\Upsilon_1\rangle = \frac{1}{\sqrt{2}} (\alpha|0\rangle (|01\rangle + |10\rangle) + \beta|1\rangle (|11\rangle + |00\rangle))$$

applying a Hadamard gate on the first qubit

$$|\Upsilon_2\rangle = \frac{1}{2} (\alpha (|0\rangle + |1\rangle) (|01\rangle + |10\rangle) + \beta (|0\rangle - |1\rangle) (|11\rangle + |00\rangle))$$

Finally, simply rearranging the terms,

$$|\Upsilon_2\rangle = \frac{1}{2} (|00\rangle (\alpha|1\rangle + \beta|0\rangle) + |01\rangle (\alpha|0\rangle + \beta|1\rangle) + |10\rangle (\alpha|1\rangle - \beta|0\rangle) + |11\rangle (\alpha|0\rangle - \beta|1\rangle))$$

Now Alice performs a measurement in the computational basis of two qubits and sends two bits to Bob via a classical communication channel telling him the outcome. Depending on this, Bob performs simply single qubit operations and retrieves the state described by eq.1.19.

1.5.3 Quantum Key Distribution

Cryptography deals with the task to exchange information between parties in a way that unwanted eavesdroppers cannot acquire any information from the message they eventually intercepted. One basic protocol for this goal is to encode the message in a not understandable way for the eavesdropper, but, in order to be understandable for the receiver, the message has also to be decoded. This can be accomplished with a key known to Alice (the sender) and Bob (the receiver) alone. The secretness of the key is also the central point in cryptography. If Alice and Bob could meet, they exchange a private key; otherwise they have to use public key distribution protocols, and entanglement turns out to be very useful. A possible entanglement-based public key distribution protocol relies on the condition Alice and Bob share initially a certain amount of entanglement, say n number of singlet

states. Then both perform a measurement of the their own qubit in the z or x basis, chosen randomly. After they announce publicly the observable they measured, but not the outcome, which results anti-correlated if the measurement was performed in the same basis: so they established their shared random key. Other QKD protocols, like the BB84, doesn't even rely on the initial entanglement sharing.

1.5.4 Entanglement and Quantum Phase Transition

Apart from being a resource for different technological devices and a central epistemological question about the nature of quantum physics, entanglement can be seen also as a methodological approach to several physical phenomena. Here we consider the relationship between entanglement and quantum phase transitions (QPT).

A QPT takes place, at zero temperature, in a many-body system when a qualitative change in its ground state occurs by tuning a parameter of the system's hamiltonian. The nature of the fluctuations in a QPT is fully quantum and at the critical point of the value of the parameter, long-range correlations appear. If these quantum long-range correlations exhibit an entanglement content is still under investigation and a general theory has, at present-days, not been proposed. Here we outline the role of entanglement in the transverse Ising model.

A well known [16][17] system undergoing QPT is the 1D XY spin $\frac{1}{2}$ model in a transverse magnetic field

$$H = - \sum_{n=0}^{N-1} \left(\sigma_z^n + \frac{\lambda}{2} \left((1 + \gamma) \sigma_x^n \sigma_x^{n+1} + (1 - \gamma) \sigma_y^n \sigma_y^{n+1} \right) \right) \quad (1.20)$$

The system described by eq.1.20 exhibits different behaviour according to the degree of anisotropy γ and the ratio of the exchange coupling and the external fields strength $\lambda = \frac{J}{h}$. For $\gamma = 1$ one obtains the transverse Ising model which is the simplest quantum lattice system undergoing a second order QPT at $\lambda = 1$, with the magnetization $\langle \sigma_x \rangle$ playing the role of the order parameter distinguishing the paramagnetic phase with $\langle \sigma_x \rangle = 0$ and $\lambda < 1$ from the ferromagnetic one where $\langle \sigma_x \rangle \neq 0$ and $\lambda > 1$. It has been shown that concurrence between nearest neighbours is maximum at the critical point where a logarithmic divergence is present for its derivative respect to λ . Furthermore, entanglement shows finite-size scaling near the critical point,

that is concurrence for finite-size systems diverges logarithmically with the number of spins N . But unlike quantum correlations between spins, which at the critical point are of infinite range, concurrence doesn't extend over next-nearest neighbours, indicating that the non-local part of the two point correlation occurring at the QPT point is not truly significant.

Chapter 2

Spin Systems

As seen in the previous chapter, entanglement generation and distribution is the main ingredient of many quantum-information tasks; therefore, as entanglement between parties is generated only through their direct interaction, entanglement or quantum state-transfer schemes are needed in almost all quantum information protocols.

Indeed, the problem of designing quantum networks which enable efficient and high-fidelity transfer of quantum states has been addressed by a number of authors, especially focusing on the requirement of minimal control. That means that state-transfer should be achieved without many control operations, such as switching on and off the interactions, measuring, encoding or decoding [18, 19, 20, 21, 22, 23, 24].

In this respect, spin systems provide ideal models to study the dynamics of quantum coherence and entanglement as they can be naturally thought as qubit registers and exploited as quantum channels (or coherent data bus). Spin chains with fixed interactions have been considered [18], and solid state implementations have been already put forward [19]. By suitable modifications of the set-up proposed by Bose in [18], it has been shown that perfect transfer can be achieved in many ways: 1) by performing local measurement at the other sites [21], 2) by using several spin chains in parallel [22], 3) by employing local memories at the receiver side [23], or 4) by means of a spatial modulation of the spin coupling strengths [24]. For this latter case, the effect of static errors in the engineering of the qubit chain has been analyzed in [25], where a scaling relation has been obtained for the transmission fidelity as a function of the degree of imperfection.

Apart from this latter example, considerable attention has been devoted

to study the effect of disorder in spin systems from the point of view of quantum information theory. Perturbative, numerical, and Bethe-Ansatz-based investigations of entanglement between two defects have been performed for a disordered anti-ferromagnetic spin-1/2 chain with anisotropic exchange coupling, [26, 27, 28]. A possibility of tuning the ground state entanglement by a single off-diagonal impurity in the anisotropic XY model has also been considered [29]. Diagonal disorder has also been considered as a mean to localize entanglement in [30]. However, the effect of the presence of defects (or, in a more solid-state oriented language, “impurities”) in the transmission of a quantum state has not been analyzed in detail

It is well known that disorder can lead to a spatial localization of the electronic wave function [31], and this occurs even if there’s only a single impurity in one and two-dimensional systems described by a tight-binding hamiltonian [32]. That’s precisely the effect that will be discussed in the following.

This chapter begins a brief overview of different spin hamiltonians, then we focus on the one-dimensional XX hamiltonian and review some of its physical implementations; next, by use of the Green’s operator formalism, we solve this system in presence of a single diagonal defect. In many of the existing physical implementations, starting from a homogeneous system, diagonal defects can be “artificially created” by controlling some external parameter, an ability which is essential to perform one-qubit gates. This amounts to discuss a chain in which the qubit level spacing is equal at every site but one. We see that this system exhibits a localized eigenstate, which can become also the ground state via a first-order quantum phase transition.

In sec.2.5 the entanglement properties of this localized ground state is analyzed. In sec.2.6 fidelity and entanglement measure are derived for our model; then, quantum-state storage and transfer are addressed, showing how the impurity site can be used both as 1.) a truly physical place to store a quantum state or entanglement with an external spin (sec.2.7) and 2.) as an entanglement mirror, where entanglement waves can be reflected backwards, sec.2.8.

Finally, another diagonal impurity is added (sec.3) to the system, which gives rise (1) to a non-zero ground-state entanglement between the two impurities; and, referring to quantum-state transmission, (2) to bouncing of entanglement between an external spin and the two impurities as well as (3) to the possibility of trapping the entanglement waves in a finite region bounded by the two defects.

2.1 Spin Hamiltonian

A general spin interaction hamiltonian of two level-systems over a lattice is

$$H = - \sum_{\mathbf{n}, \mathbf{m}; \alpha, \beta} J_{\mathbf{n}\mathbf{m}}^{\alpha\beta}(t) \sigma_{\alpha}^{\mathbf{n}} \sigma_{\beta}^{\mathbf{m}} \quad (2.1)$$

where J is the exchange coupling, σ 's are the Pauli matrices, α, β runs over the cartesian axes x, y, z and \mathbf{n}, \mathbf{m} are the spin position labels on the lattice. This kind of hamiltonian describes a great variety of physical systems with properties changing dramatically as the type or the dimensionality of the lattice, the strength of the coupling or other parameters varies.

If one considers a vector-like, time-independent, nearest-neighbours and homogeneous interaction between spins, eq.2.1 reduces to the class of Heisenberg hamiltonian [33]

$$H = - \sum_{\langle \mathbf{nm} \rangle; \alpha} J^{\alpha} \sigma_{\alpha}^{\mathbf{n}} \sigma_{\alpha}^{\mathbf{m}} \quad (2.2)$$

where $\langle \cdot \rangle$ denotes next-neighbours sites. Because of the magnetic origin of this hamiltonian, the coupling $J > 0$ is said ferromagnetic, as it tends to align parallel spins, while $J < 0$ anti-ferromagnetic.

Even if this hamiltonian is innocent looking, nevertheless is it a formidable task to solve it analytically. The reason is that the spin operators are neither bosons nor fermions, in fact they obey peculiar commutations rules

$$[\sigma_x^n, \sigma_y^m] = 2i\epsilon^{ijk} \sigma_k^n \delta_{nm}$$

To show this point in more detail let's introduce raising and lowering operators at each lattice site

$$\begin{cases} \sigma_+ = \frac{\sigma_x + i\sigma_y}{2} \\ \sigma_- = \frac{\sigma_x - i\sigma_y}{2} \end{cases}$$

If we denote the two spin states as $|0\rangle$ and $|1\rangle$, their action is to increase (decrease) by one unit the z quantum number of the spin

$$\begin{aligned}\sigma_+|1\rangle &= |0\rangle & \sigma_+|0\rangle &= 0 \\ \sigma_-|1\rangle &= 0 & \sigma_-|0\rangle &= |1\rangle\end{aligned}$$

and the following commutation relations hold

$$[\sigma_+^n, \sigma_-^m] = \sigma_z^n \delta_{nm} \quad [\sigma_z^n, \sigma_+^m] = 2\sigma_+^n \delta_{nm} \quad [\sigma_z^n, \sigma_-^m] = -2\sigma_-^n \delta_{nm}$$

so that the operators satisfy boson commutation rules on different sites, but on the same site they behave like fermions

$$\{\sigma_+^n, \sigma_-^n\} = 1$$

For 1D spin arrays with isotropic exchange coupling, that is $J_x = J_y = J_z$, a solution of eq.2.2 can be found using the Bethe-Ansatz. It's applicability relies on two symmetries of the hamiltonian: the rotational and the translational one. The first one reflects the invariance of the hamiltonian with respect to continuous rotations around the z axis and implies the conservation of z component of the total spin along the same direction, the second one involves the invariance of the hamiltonian by discrete translation of any number of lattice spacing and implies that the eigenstates of the hamiltonian have to be also eigenvectors of the momentum operator. For coupling constants which differs along the axis, Bethe-Ansatz is still a valid technique if the two symmetries hold, i.e. the XXZ and the XX model¹ and the Ising model where $J_x = J_y = 0$, even if one adds an uniform external magnetic field along some direction. On the contrary, for the XY and XYZ model Bethe-Ansatz cannot be used because of the absence of the rotational symmetry. In the XY case ($J_x \neq J_y, J_z = 0$) a diagonalization technique, involving the Jordan-Wigner transformation, permits to reduce the hamiltonian to that of spinless non-interacting fermions, thus easy to diagonalize, even in presence of an uniform external magnetic field [34].

If we go to higher dimensions the eigenvalue problem given by the hamiltonian of eq.2.2 becomes considerably more difficult to solve. If we deal with an Ising model a solution, without any additional magnetic field, was given

¹the different hamiltonians arising from the Heisenberg model will be denoted in the following with capital letters along the axis where the interaction between spins is present, and in the case where it is equal the letter is repeated.

by Onsager for 2D systems; for the XXZ and the XX model generalized Jordan-Wigner transformation permits to solve the eigenvalue problem for every lattice dimensionality [35][36].

Henceforth we refer to the 1D XX model, with ferromagnetic coupling, placed in an external magnetic field h overall uniform and we assume periodic boundary conditions (that is the last spin identifies with the first one, $\sigma^{\frac{N}{2}} = \sigma^{-\frac{N}{2}}$):

$$H = -h \sum_{n=-\frac{N}{2}}^{\frac{N}{2}-1} \sigma_z^n - J \sum_{n=-\frac{N}{2}}^{\frac{N}{2}-1} (\sigma_x^n \sigma_x^{n+1} + \sigma_y^n \sigma_y^{n+1})$$

in the $\{\sigma_+, \sigma_-, \sigma_z\}$ representation (the summation henceforth is intended over the same range, if not otherwise reported)

$$H = -h \sum_n \sigma_z^n - 2J \sum_n (\sigma_+^n \sigma_-^{n+1} + \sigma_-^{n+1} \sigma_+^n) \quad (2.3)$$

The physics of this hamiltonian is well known; translational invariance and rotational symmetry around z direction allows the use of the Bethe Ansatz. So eq.2.3 can be diagonalized in the invariants Hilbert subspaces \mathcal{H}_m , with m giving the number of excitations, i.e. spin reversed along the z direction, therefore the solution space is given by $\mathcal{H}_{sol} = \oplus^m \mathcal{H}_m$ (fig.2.1), with

$$\mathcal{H}_0 = \underbrace{\{|000\dots 00\rangle}_{N}} \equiv \{|0\rangle} \quad (2.4)$$

$$\mathcal{H}_1 = \underbrace{\{|100\dots 00\rangle}_{N}, \underbrace{|010\dots 00\rangle}_{N}, \dots} \equiv \{|n\rangle} \quad (2.5)$$

$$\vdots \quad \quad \quad \vdots \quad \quad \quad (2.6)$$

$$\mathcal{H}_N = \underbrace{\{|111\dots 11\rangle}_{N}} \equiv \{|N\rangle} \quad (2.7)$$

where $|n\rangle$ denotes the $n - th$ spin reversed in the ring.

In \mathcal{H}_0 there is only one eigenstate given by $|0\rangle^{\otimes N}$, with $E_0 = -Nh$. It corresponds to a state with all spin pointing in the positive z direction.

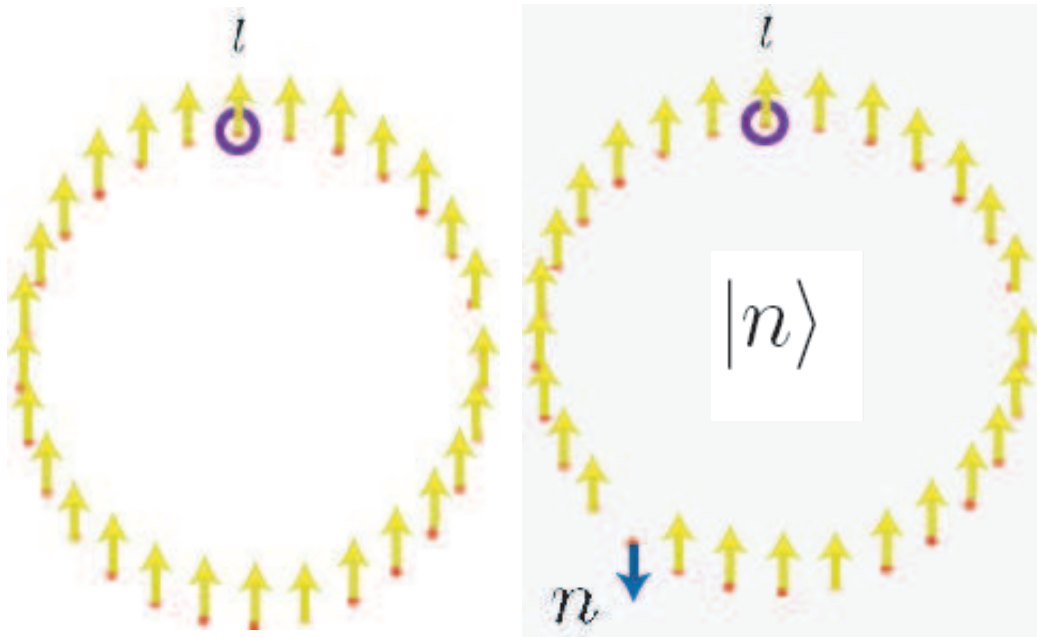


Figure 2.1: (left) Hilbert space \mathcal{H}_0 has only one state where all spins are pointing in the same direction (the quantization axis given by the applied magnetic field); (right) Hilbert space \mathcal{H}_1 has as many states as the number of spins; each state is expressed in the computational basis by $|n\rangle$, referred to the state with the n -th spin reversed. The spin l refers to the site on which, in the next section, an inhomogeneity will be placed.

In the Hilbert space sector \mathcal{H}_1 where one spin is pointing downwards, the eigenstates are given by

$$|k\rangle = \frac{1}{\sqrt{N}} \sum_n e^{\frac{2\pi i k n}{N}} |n\rangle$$

where $|n\rangle$ indicates that the spin labeled by n is in the $|1\rangle$ state. These eigenstates represents plane waves and usually are referred to as magnons, whose energy is $E_k = -(N-2)h - 4J \cos(\frac{2\pi k}{N})$ with k running from $-\frac{N}{2}$ to $\frac{N}{2}$ by unit steps². In this Hilbert subspace the hamiltonian 2.3 is equivalent to a tight-binding model.

In the thermodynamic limit, the system exhibits a quantum phase transition (QPT), driven by the dimensionless coupling $\gamma = \frac{h}{2J}$. For $\gamma < 1$ the ground state is given by $|0\rangle^{\otimes N}$, but, for γ equal to its critical value of 1, the ground state becomes degenerate because the state $|0\rangle^{\otimes N}$ and the state $|k=0\rangle = \frac{1}{\sqrt{N}} \sum |n\rangle$, belonging to the Hilbert space sector of one excitation, have the same energy. For $\gamma > \gamma_c$ the ground state involves many-excitations sectors of the Hilbert space.

2.2 1D Spin Chain with Defects

Now we introduce a diagonal defect in the ring structure, that is we change the uniform external magnetic field along the z axis by an amount ϵ_i on the i -th site. The new hamiltonian is

$$H = -h \sum_n \sigma_z^n - J \sum_n (\sigma_x^n \sigma_x^{n+1} + \sigma_y^n \sigma_y^{n+1}) - \sum_i \epsilon_i \sigma_z^i \quad (2.8)$$

which can be written in the subsequent form, reminding that $\sigma_+^i \sigma_-^i = |i\rangle\langle i|$

$$H = -h \sum_n \sigma_z^n - 2J \sum_n (\sigma_+^n \sigma_-^{n+1} + \sigma_+^{n+1} \sigma_-^n) + \sum_i \epsilon_i - 2 \sum_i \epsilon_i \sigma_+^i \sigma_-^i \quad (2.9)$$

Rotational symmetry still holds for this hamiltonian, so the z -component of the total spin continues to be conserved and the structure of the solution's

²As we will go over $N \rightarrow \infty$, we have set $N-1 \rightarrow N$ in the previous expressions.

Hilbert space is the same as for the hamiltonian of eq.2.3; but translational symmetry is broken and therefore the eigenstates of eq.2.3 are no more eigenstates of the defected hamiltonian. Before presenting the solution of the new eigenvalue problem, a few physical systems described by this kind of hamiltonian are presented and, as Green's operators technique will be employed, a brief overview of their properties is given.

2.2.1 Physical Systems Described by the Hamiltonian

Several different physical systems are described by the hamiltonian of eq.2.9 (or reduce to it in the subspace \mathcal{H}_1 , where an additional interaction $J_z \sigma_z^n \sigma_z^{n+1}$ produces only an irrelevant energy shift) and some of them are also experimentally realizable with present-day technologies.

In [19] a 1D Josephson junctions [37] array is presented in which the qubit is represented by the a Cooper pair box, fig.2.2, and a recently realized super-conducting tunnel junction circuit [38] exhibits also the possibility to control single qubits dynamics, so that diagonal defect control, described by the last term in the hamiltonian 2.9, can be achieved. A Josephson junction array of length L is described by an hamiltonian

$$H = \frac{1}{2} \sum_{ij}^L (Q_i - Q_{xi}) C_{ij}^{-1} (Q_j - Q_{xj}) - E_J \sum_i^{L-1} \cos(\phi_i - \phi_{i+1}) \quad (2.10)$$

where the first term is the charging energy due to the applied voltage, with Q_i the charge of the i -th junction and C_{ij} the capacitance matrix, the second term accounts for the tunneling of the Cooper pair. In the regime $e^2 C_{00}^{-1} \gg E_J$ the hamiltonian 2.10 reduces to the XXZ spin- $\frac{1}{2}$ model [39].

Another possibility is to use cold atoms in optical lattices. In the last decades laser techniques advances, such as laser cooling of Fermi and Bose gases, atoms and ions trapping and many else, permits to realize physical systems accurately described by spin-type hamiltonians[40]. The experimental protocol of these techniques starts by trapping the atomic gas with magneto-(optical) devices and then superimpose on the trap the lattice potential generated by the lasers. Atomic systems in optical lattices presents the advantage with respect to solid-state devices of the precise knowledge of the model hamiltonian, manipulation of its coupling constants and generation of controllable disorder, in addition of the possibility to realize a great

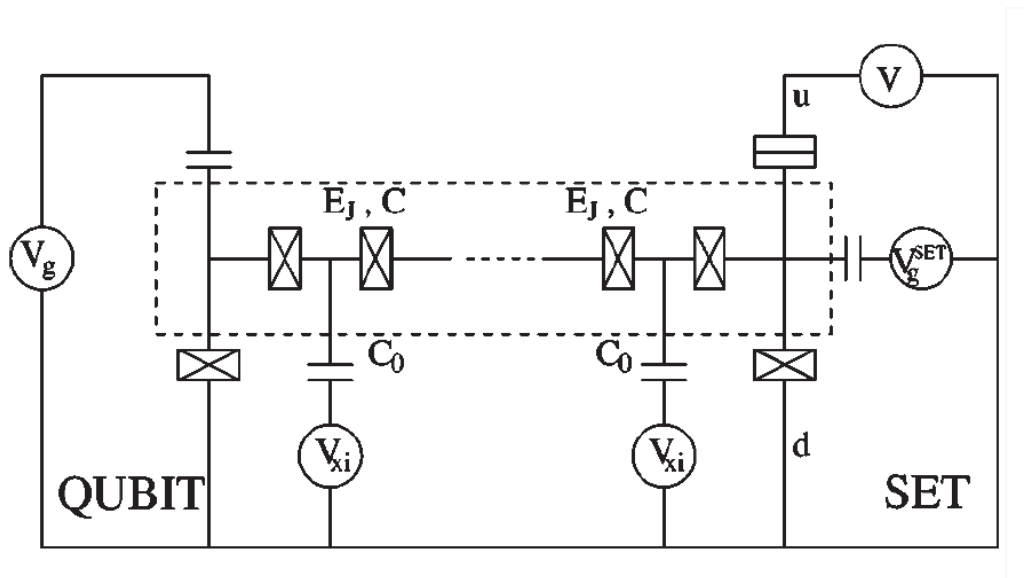


Figure 2.2: Dashed box: one-dimensional Josephson array proposed for the transmission of quantum states. The crossed rectangles denote the Josephson junction between the islands. The state prepared on the left-most island is transferred to the right by the time evolution generated by the hamiltonian. On the left and the right are present respectively the Cooper-pair box used to prepare the state and the measurement device.

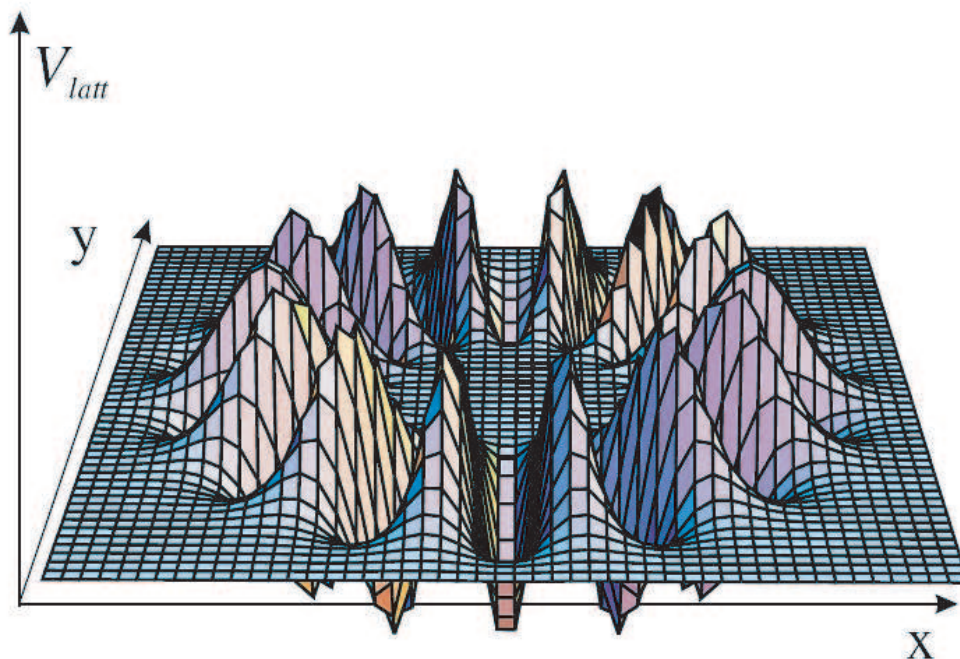


Figure 2.3: The optical potential resulting from the interference of a plane wave with a LG mode in which 14 sites has been realized.

variety of different optical lattices. In [41], for example, a perfect 1D ring has been obtained by interference of a plane wave with Laguerre-Gauss laser modes, fig.2.3, and, loading fermionic atoms into this optical ring-shaped lattice, realizes an hamiltonian that, by tuning the laser frequencies within the atomic fine structure, reduces also to the XXZ model. Starting from Bose-Einstein condensates (BEC) it has been possible to store approximately up to two atoms per site.

Another experimental implementation of the hamiltonian 2.9 has been realized with electrons floating on a liquid helium thin surface [42].

2.3 Green's Function

The use of Green's operators turns out to be very useful in many ways, here we discuss only their application in a context where the hamiltonian is time-independent and the results connected to the Dyson series. Green's operator is defined by

$$(z - L)G(z) = 1 \quad (2.11)$$

where z is a complex number, L is a linear, time-independent hermitian operator, which we shall assume to be the hamiltonian, and $G(z)$ is its Green's operator. In the position-representation definition 2.11 reads as a inhomogeneous differential equation

$$(z - L(r))G(r, r'; z) = \delta(r - r') \quad (2.12)$$

In the following the hamiltonian operator H is assumed to have a complete set of eigenvectors $\{|\psi_k\rangle\}$, with eigenvalues $\{E_k\}$, where the index k can assume both discrete and continuous values.

Solving eq.2.11 formally one obtains, if $z \neq \{E_k\}$

$$G(z) = \frac{1}{z - H} = \sum_k \frac{|\psi_k\rangle\langle\psi_k|}{z - E_k} + \int dk' \frac{|\psi_{k'}\rangle\langle\psi_{k'}|}{z - E_{k'}}$$

where in the last equation the so-called eigenfunction decomposition technique has been used with k and k' referring respectively to the discrete and the continuous spectrum of H . From this last equation one sees that $G(z)$ is analytic in the complex- z plane except for two cases:

- at the points where z is equal to a discrete eigenvalue E_k ;
- at the portions of the real axis where z equals $E_{k'}$.

In the first case the simple poles of $G(z)$ give the discrete eigenenergies of H and information about the corresponding eigenvectors can be found computing the residue at $z = E_k$

$$Res[G(z), E_k] = \sum_i |\psi_i\rangle\langle\psi_i| \quad (2.13)$$

with the summations running over the degeneracy of the eigenvalue E_k .

In the second case Green's operator is not well defined cause of the presence of the pole in the integrand, but one can use a limiting procedure

$$G^\pm(z) = \lim_{\epsilon \rightarrow 0^+} G(z \pm i\epsilon) \quad (2.14)$$

The two limits exist but are not the same, so the continuous spectrum is revealed by a branch cut, I_b , along the real axis in the z plane. The corresponding eigenvectors are delocalized in the space domain, i.e. they don't decay with $r \rightarrow \infty$.

It is also possible that the two side limits defined by eq.2.14 don't exist, then the corresponding singularities on the real axis denote a so-called natural boundary and the corresponding eigenstates are localized. As in our work we encounter the first situation, we briefly outline the description of the construction of the extended eigenvectors in the case we wish to solve the following eigenvalue problem

$$(E - H)|\psi(E)\rangle = 0 \quad (2.15)$$

where E belongs to the branch cut.

To accomplish this task some elements of time-independent perturbation theory are required, leading to the Dyson series expansion. We assume that H in eq.2.15 can be written in the form $H = H_0 + H_I$, and that a spectral decomposition of H_0 is given. So Dyson expansion of the Green's operator G of the full hamiltonian H in terms of H_I and the Green's operator of H_0 is

$$G = G_0 + G_0 H_I G_0 + G_0 H_I G_0 H_I G_0 + \dots = G_0 + G_0 H_I G = G_0 + G H_I G_0 \quad (2.16)$$

Frequently, when dealing with scattering processes for instance, it is useful to introduce the so-called T matrix, whose definition is

$$\begin{cases} T(z) = H_I G(z)(z - H_0) & z \notin I_b \\ T^\pm(z) = H_I G^\pm(z)(z - H_0) & z \in I_b \end{cases} \quad (2.17)$$

Also for the T matrix a Dyson expansion is possible and gives

$$T(z) = H_I + H_I G_0 H_I + H_I G_0 H_I G_0 H_I \cdots = H_I + H_I G H_I = H_I + H_I G_0 T = H_I + T G_0 H_I \quad (2.18)$$

Finally the relation between the Green operator of the full hamiltonian and the T matrix is given by

$$G(z) = G_0(z) + G_0(z)T(z)G_0(z) \quad (2.19)$$

From this last expression it is evident that, under the condition that $G_0(z)$ is known, the T matrix fully determines the Green operator. In fact, they have the same analytical structure, so that the poles and the branch cuts of T have the same meaning as those of G .

With these new instruments we can now face the problem of the determination of the continuous eigenstates

$$|\Psi^\pm\rangle = |\psi_{k'}\rangle + G_0^\pm T^\pm |\psi_{k'}\rangle = |\psi_{k'}\rangle + G^\pm H_I |\psi_{k'}\rangle \quad (2.20)$$

where the \pm sign refers to eigenstates obtained using the corresponding G^\pm operator and accounts for different physical processes, like in scattering where the minus sign solution is excluded as representing meaningless ingoing spherical waves towards the scattering center.

2.4 The XX Model with One Defect

In the framework of Green operator perturbation theory we can now find the spectral resolution of the hamiltonian given by eq.2.9 when only a single defect is present at $l = 0$, with some constant factors re-scaled for further convenience and the coupling constant J set as energy unit

$$H_0 = -\frac{\omega_0}{2} \sum_n \sigma_z^n - \sum_n (\sigma_+^n \sigma_-^{n+1} + \sigma_-^{n+1} \sigma_+^n) + \frac{\alpha}{2} \quad (2.21)$$

$$H_I = -\alpha \sigma_+^l \sigma_-^l \quad (2.22)$$

The solution of the unperturbed hamiltonian (eq.2.21) presents the same structure of solution's Hilbert space as given by eq.2.3, and the effect of

the last term is only an energy shift by $\frac{\alpha}{2}$ upon the eigenvalues with the eigenvectors left unchanged. Without loss of generality, we re-scale $E_0 = \frac{-N\omega_0 + \alpha}{2}$ to zero, so that in the one-excitation sector we have $E_1 = \omega_0 - \cos \frac{2\pi k}{N}$.

The mechanism outlined in sect.2.3 requires initially the Green operator for the unperturbed hamiltonian

$$G_0(z) = \frac{1}{z - H_0} = \sum_k \frac{|k\rangle\langle k|}{z - E_k} \quad (2.23)$$

In the thermodynamic limit, $N \rightarrow \infty$, $L \rightarrow \infty$ and $\frac{N}{L} = \text{const}$, the discrete index $k = \frac{2\pi}{N}$ becomes continuous and the discrete levels merge into a continuous band: $E(k) \in [\omega_0 - 1, \omega_0 + 1] = I_b$, which is revealed by the branch cut on the real axis in the z -complex plane.

Now we can write down explicitly the matrix element of G_0 in the computational basis of \mathcal{H}_1

$$G_0(r, s; z) = \frac{1}{2\pi} \int_{-\pi}^{\pi} d\theta \frac{\exp[i\theta(r-s)]}{z - \omega_0 + \cos \theta} = \begin{cases} G_0(r, s; z) = \frac{(-x + \sqrt{x^2 - 1})^{|r-s|}}{\sqrt{x^2 - 1}} & z \notin I_b \\ G_0^\pm(r, s; z) = \frac{(-x \pm i\sqrt{1-x^2})^{|r-s|}}{\pm i\sqrt{1-x^2}} & z \in I_b \end{cases} \quad (2.24)$$

where $x = z - \omega_0$.

Taking into account the perturbation H_I of eq.2.21, and using expressions 2.18 and 2.16, the right-hand side terms can be re-summed exactly due to the diagonal form of H_I in the one-excitation sector

$$T(z) = |l\rangle \frac{\alpha}{1 + \alpha G_0(l, l; z)} \langle l| = |l\rangle t_l \langle l| \quad (2.25)$$

$$G(z) = G_0(z) - G_0(z)T(z)G_0(z) \quad (2.26)$$

The matrix elements of the G operator can be also represented by Feynmann diagrams, making sense to the term "propagator" referred to G , fig.2.4.

As the branch cut of $G(z)$ is the same as for the unperturbed Green operator, eq.2.26, the continuous band is unaffected by the presence of the impurity, therefore still it is located in the interval $E \in [\omega_0 - 1, \omega_0 + 1]$. The use of eq.2.20 enable us to retrieve the eigenstates expanded in the c.b.

$$|\Psi(E)\rangle = \sum_n a_n(E) |n\rangle \quad (2.27)$$

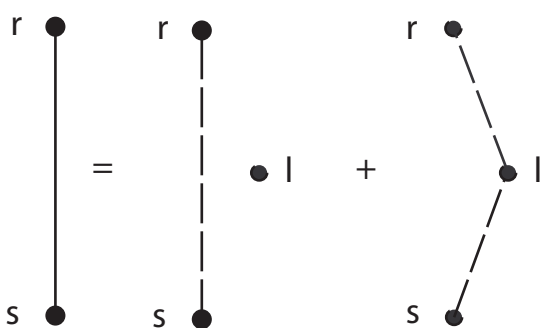


Figure 2.4: The matrix element $G(r, s; z) = G_0(r, s; z) + G_0(r, l; z)t_l G_0(l, s; z)$ is the sum of the free propagation of the excitation from site s to r (first right-side diagram) and the free propagation from s to l , where scattering take place, then again free propagation from l to r .

where the probability amplitudes of finding the n -th spin reversed is given by

$$a_n(E) = \frac{1}{\sqrt{N}} \left(e^{i\theta n} - \frac{\alpha e^{i|\theta||n-l|}}{i \sin |\theta| + \alpha} e^{i\theta l} \right), \quad (2.28)$$

and $\cos \theta = \omega_0 - E$.

Besides a distortion of the states within the band, the perturbation produces the appearance of a discrete eigenstate, whose energy is given by the simple pole of the Green function 2.26, determined by the equation $1 + \alpha G_0(l, l; z) = 0$. This state lies below or above the band (as for $E \in I_b$ the Green function has also an imaginary part) depending on whether α is greater than zero or not, and its energy is $E_{loc} = \omega_0 \mp \sqrt{1 + \alpha^2}$. Explicitly, the state is given by $|\Psi(E_{loc})\rangle = \sum_n b_n(E_{loc})|n\rangle$, with

$$b_n = \begin{cases} -\frac{\sqrt{|\alpha|}}{(1+\alpha^2)^{\frac{1}{4}}} \exp[-\xi(\alpha)|n-l|] & \alpha > 0 \\ (-1)^{|n-l|} \frac{\sqrt{|\alpha|}}{(1+\alpha^2)^{\frac{1}{4}}} \exp[-\xi(\alpha)|n-l|] & \alpha < 0 \end{cases}$$

where

$$\xi(\alpha) = -\ln \left(\sqrt{1 + \alpha^2} - |\alpha| \right) \quad (2.29)$$

As one can see directly from this expression, the spin excitation is exponentially located near the defect, with a localization length, given by ξ^{-1} , which characterizes the spatial extension of the wave function around site l . This characteristic length goes logarithmically to zero with increasing α , but is already less than the site spacing for a defect strength of the same order of the ferromagnetic coupling (to be more precise, we have $\xi^{-1} < 1$ for $\alpha \geq (1 - e^2)/2e \simeq 1.175$).

Moreover there is also a first-order quantum phase transition (QFT) for

$$\alpha \geq \sqrt{\omega_0^2 - 1} \quad \text{and} \quad \omega_0 > 1$$

as for these values of the hamiltonian's parameters, the energy (at temperature $T = 0$) of the localized state is less than that of the $|0\rangle$ state and becomes the new ground state.

Let's illustrate this point in more detail. In sec.2.1 it was shown that the 1D XX spin- $\frac{1}{2}$ ring in transverse field has the (only) state in the zero-excitation sector as its ground state, namely $|GS\rangle = |0\rangle$, for $\omega_0 > 1$. Adding an impurity $\alpha > 0$ (and performing an irrelevant global energy shift so that the energy of the zero-excitation and one-excitation states were left unchanged), a localized level appears with energy $E_{loc} = \omega_0 - \sqrt{1 + \alpha^2}$. This energy becomes less than the energy of the $|0\rangle$ state if $\alpha > \sqrt{\omega^2 - 1}$, therefore the localized state $\Psi(E_{loc})$ becomes the new ground state:

$$|GS\rangle = \begin{cases} |0\rangle^{\otimes N} & \alpha < \alpha_c & E_{GS} = 0 \\ |\Psi(E_{loc})\rangle & \alpha > \alpha_c & E_{GS} = \omega_0 - \sqrt{1 + \alpha^2} \end{cases}$$

with the critical value of the impurity given by $\alpha_c = \sqrt{\omega^2 - 1}$

To evaluate the order of the QPT, we take the derivatives of the energy respect to α at α_c :

$$\begin{cases} \frac{\partial E_{GS}}{\partial \alpha} \Big|_{\alpha=\alpha_c^-} = 0 \\ \frac{\partial E_{GS}}{\partial \alpha} \Big|_{\alpha=\alpha_c^+} = \frac{1+\omega_0^2}{\omega_0} \end{cases}$$

because of the discontinuity of the 1-th order derivative of the energy at the critical point, the system exhibits a 1-th order QPT, which doesn't present spontaneous symmetry breaking phenomena.

2.5 Ground-State Entanglement

We analyze the entanglement content shared by two qubits located at i and j , when the ground state is the localized one. The concurrence turns out to be [43]

$$C_{ij} = 2|(G(i, j; E_{loc})| = \frac{2|\alpha|e^{-\xi(|i|+|j|)}}{\sqrt{1 + \alpha^2}} \quad (2.30)$$

From this equation it follows that two qubits are entangled only if the sum of their distance from the defect doesn't considerable exceed the localization length ξ^{-1} defined by eq.2.29. In that sense we state that entanglement

is localized around the impurity site in the localized ground state of the system, fig.2.5. In analogy with the Ising model in transverse field [16], below the critical value of α the ground state is a product state as well as for $\alpha \rightarrow +\infty$, but at the critical value entanglement is present between spins in the neighbourhood of the impurity.

2.6 Fidelity and Concurrence in our Model

The solution of the Schrödinger equation reported in the previous section enables us to describe our system by means of a density matrix, which, in turns, permits to obtain analytic quantities for the fidelity and the concurrence of sec.1.3.2 and 1.4.1. In both cases we analyze the effect of the impurity on transmission's tasks in the paramagnetic phase of the ring, that is when $\omega_0 > 1$. This last requirement is due to the necessity of choosing the $|0\rangle$ state as ground state of the system because we want essentially to send an excitation along the chain remaining in the one-excitation sector of the Hilbert space.

Let's start with the situation where initially an unknown quantum state is put on the spin s (sender) with the rest of the chain in the factorized ground state

$$|\Psi(t=0)\rangle = (a|0\rangle + b|s\rangle) |0\rangle^{\otimes N-1} \quad (2.31)$$

Then the pure state of the whole ring at time t is given by

$$|\Psi(t)\rangle = a|0\rangle + b \sum f_{sn}(t)|n\rangle \quad (2.32)$$

where $f_{sn} = \langle n|^{-iHt}|s\rangle$ is the transition amplitude of the excitation from spin s to n . The density matrix of an arbitrary spin r , which will be generally in a mixed state, is obtained via the partial trace over the total density matrix

$$\rho^{(r)}(t) = \begin{pmatrix} 1 - |b|^2|f_{rs}(t)|^2 & ab^*f_{rs}^*(t) \\ a^*bf_{rs}(t) & |b|^2|f_{rs}(t)|^2 \end{pmatrix} \quad (2.33)$$

Using eq.1.18 the quality of the transmission is

$$\langle F(t) \rangle = \frac{1}{2} + \frac{|f_{rs}(t)|^2}{6} + \frac{Re[f_{rs}(t)]}{3}$$

With an appropriate choice of the qubit level spacing ω_0 the last term can be maximized and the fidelity results

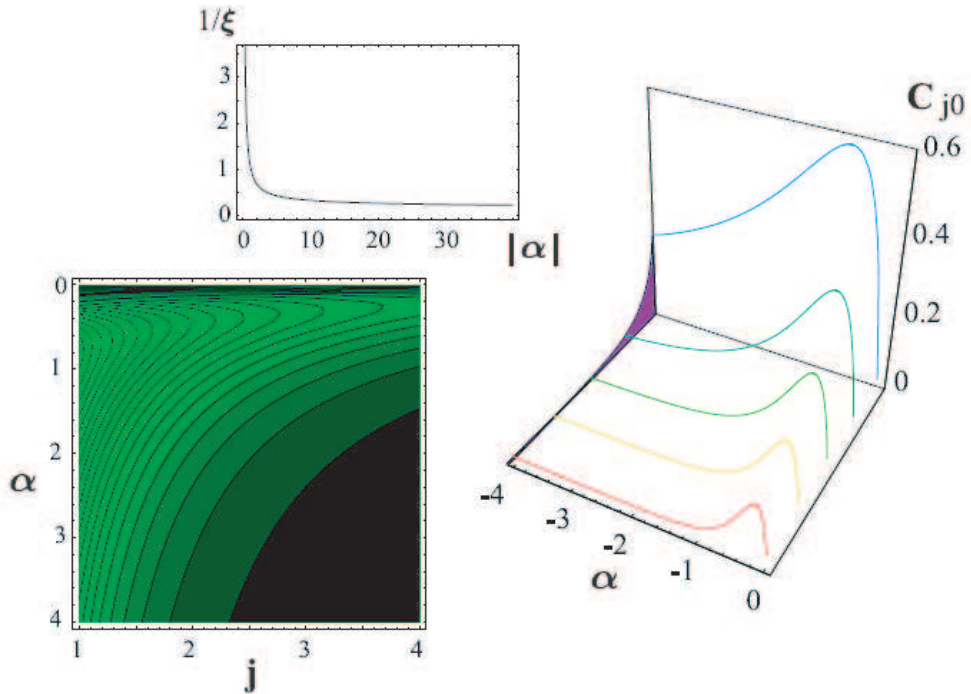


Figure 2.5: (up-left) Localization length as a function of α . (down-left and right) Ground-state concurrence between the impurity and the spin at site j . Notice the exponential decrease as a function of the distance.

$$\langle F(t) \rangle = \frac{1}{2} + \frac{|f_{rs}(t)|^2}{6} + \frac{|f_{rs}(t)|}{3} \quad (2.34)$$

On the other end, to send entanglement over the chain, one prepares an initial state in which the spin s is entangled with an external spin e , i.e. uncoupled from the chain and therefore not involved in the evolution determined by the hamiltonian, with the rest of the chain always in the ground state $|0\rangle$

$$|\Psi(t=0)\rangle = \frac{1}{\sqrt{2}} (|1_e 0\rangle + e^{i\phi} |0 - e s\rangle) |0\rangle^{\otimes N-1} \quad (2.35)$$

where the relative phase ϕ accounts for all one-excitation maximal entangled states, i.e. from the singlet at $\phi = \pi$ to the triplet at $\phi = 0$. The aim is then to swap the state of the sender and the receiver, in order to transfer the initial entanglement between s and e to r and e . The success of this operation is measured by the concurrence (sec.1.3.2), whose explicit expression is computed via the two-qubit density matrix

$$\rho^{(er)}(t) = \frac{1}{2} \begin{pmatrix} 1 - |f_{rs}(t)|^2 & 0 & 0 & 0 \\ 0 & 1 & e^{i\phi} f_{rs}(t) & 0 \\ 0 & e^{-i\phi} f_{rs}^*(t) & |f_{rs}|^2 & 0 \\ 0 & 0 & 0 & 0 \end{pmatrix} \quad (2.36)$$

and the concurrence is simply

$$C_r = |f_{rs}(t)| \quad (2.37)$$

In presence of the defect, the transition amplitude is

$$f_{rs}(t) = b_r b_s^* e^{-iE_{loc}t} + \int_{\omega_0-1}^{\omega_0+1} dE a_r(E) a_s^*(E) \quad (2.38)$$

The first contribution to f_{rs} comes from the localized state and describes an information transport mediated by $|\Psi_{loc}\rangle$. It has a spatially localized (i.e. exponentially decaying) structure, so that it can be neglected when $|r-s| > \xi^{-1}$, while it constitutes the dominant term when sender and receiver are near to each other (and, in particular, for the case of information storage, see sec.2.7).

The second contribution is an integral over the branch cut region of the Green function and describes an information transport mediated by the states

within the continuous band. When $\alpha \rightarrow 0$, it reduces to the unperturbed transition amplitude, given by the Bessel function of order $r-s$, $J_{r-s}(t)$, [43], which can be interpreted as a spin-wave mediated information transfer, see [44]. The main effect of a finite impurity field α is to break the translation invariance of the system. This implies that the elementary excitations cannot be interpreted as magnons anymore, although their energy stays still within the same continuous band. A close examination of the second term in the amplitude shows that the defect produces a distortion of the unperturbed spin waves, which are no longer freely propagating but rather are scattered at the defect during propagation from s to r .

Eq.2.39 can be written in terms of Green's functions,

$$f_{rs}(t) = \int_{-\pi}^{\pi} \frac{d\theta}{2\pi} \left\{ e^{i\theta(r-s)} + e^{i\theta(l-s)} g_{r,l}^{(+)} + e^{i\theta(r-l)} g_{l,s}^{(-)} + g_{r,l}^{(+)} g_{l,s}^{(-)} \right\} e^{-iEt} + \text{Res}[G(r, s; E_{loc})] e^{-iE_{loc}t} \quad (2.39)$$

where, within the integral, $E = \omega_0 - \cos \theta$, while

$$g_{i,j}^{(\pm)}(E) = \frac{\alpha G_0^{(\pm)}(i, j; E)}{1 + \alpha G_0^{(\pm)}(l, l; E)} = \frac{-\alpha e^{\pm i|\theta||i-j|}}{\pm i \sin |\theta| + \alpha} \quad (2.40)$$

and then expanded asymptotically in powers the reciprocal defect strength, $1/\alpha$

$$f_{rs}(t) = \sum_n \binom{-1/2}{n} \frac{1}{\alpha^{2n}} e^{-iE_{loc}t} + (-i)^{r-s} J_{r-s}(t) - i^{r+s} J_{r+s}(t) \quad (2.41)$$

$$- \sum_{n \text{ odd}} \left(\frac{i}{2\alpha} \right)^n \sum_{k=0}^{\frac{n-1}{2}} \binom{n}{k} (J_{|r|+|s|+n-2k}(t) + J_{|r|+|s|-n+2k}(t))$$

$$+ \sum_{n \text{ even}} \left(\frac{i}{2\alpha} \right)^n \left(\sum_{k=0}^{\frac{n}{2}-1} \binom{n}{k} (J_{|r|+|s|+n-2k}(t) + J_{|r|+|s|-n+2k}(t)) + \binom{n}{\frac{n}{2}} J_{|r|+|s|}(t) \right)$$

In the next two sections we characterize the quantum-information transmission first when the initial state involves the impurity then when it doesn't, and reveal the utility of the defect both in storing and in reflecting a given state.

2.7 Information Storage

Information storage in a spin chain has been considered previously, and the case of a Heisenberg chain working as a quantum memory has been discussed, [45]. Here, instead, we will discuss an information storage that is realized by exploiting the Anderson localization phenomenon. In fact, the appearance of a localized eigenstate leads naturally to the question if it can be used to store locally quantum information and with which degree of fidelity versus time evolution. We will face this question in the limit $\alpha \gg 1$ where the localization length goes to zero, and therefore the localized state is really concentrated on the impurity site. This suggests that a high fidelity storage of information (both of single qubit states and of pairwise entanglement) can be achieved at this site. We explore this possibility in the following, trying to characterize the quality of the storage in terms of the amount of information that is lost.

Simple approximate expressions for the fidelity of storage and for the amount of stored entanglement are obtained if we limit ourselves to second order in the $1/\alpha$ expansion for the transition amplitude. From eq.2.41 for $r = s = 0$ the amplitude f_{00} has two distinct contributions: 1) the localized state gives a term of the form

$$f_{00}^{(loc)} \simeq \left[1 - \frac{1}{2\alpha^2} \right] e^{-iE_{loc}t},$$

whereas, 2) the continuous energy eigenstates give:

$$f_{00}^{(cont)} \simeq -\frac{1}{2\alpha^2}(J_0(t) + J_2(t)).$$

This latter contribution is negligible after a few exchange times due to the decay of the Bessel functions. As a result, if the sender resides at the defect, quantum information doesn't propagate at all and for the fidelity and the concurrence we obtain the simple forms (valid for $s = l = 0$):

$$F_r \simeq \begin{cases} 1 - \frac{1}{3\alpha^2} & r = 0 \\ \frac{1}{2} + \frac{r}{3\alpha t} J_r(t) & r \neq 0 \end{cases} \quad C_r \simeq \begin{cases} 1 - \frac{1}{2\alpha^2} & r = 0 \\ \frac{r}{\alpha t} J_r(t) & r \neq 0 \end{cases} \quad (2.42)$$

These results are easily interpreted: quantum information is localized at the defect site as the state $|l\rangle$ approximately coincides with the localized eigenstate $|\Psi_{loc}\rangle$. Indeed, the fidelity of storage (i.e., the fidelity for a retrieval

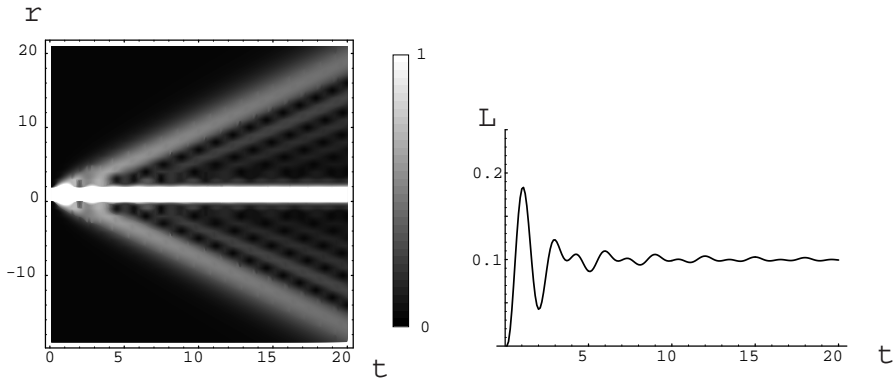


Figure 2.6: Left panel: space-time evolution of the concurrence C_r for $\alpha = 3$ with $s = l = 0$. The entanglement with the external qubit stays localized at the sender site. Right panel: time evolution of the leakage, as defined in Eq. (2.43)

at the very same site in which information was put) approaches 1 up to second order terms in $1/\alpha$. The same occurs for the case of the entanglement, as the concurrence is very high when the receiver coincides with the sender (and the defect). On the other hand, if one tries to retrieve the information at a different site, the result is very poor as the fidelity goes to $1/2$ and the concurrence goes to zero, decreasing with the distance, with time, and with increasing α . Figures 2.6 and 2.7 show that these results can be obtained even for moderate values of the defect strength. Indeed, for $\alpha = 3$, one can see that both the fidelity and the concurrence are extremely peaked at the sender site. The secondary V-shaped propagation lines are essentially a reminiscence of the unperturbed problem. In fact, for $\alpha = 0$ these would be the only existing lines, describing the distribution of information along the chain as a result of the spin wave propagation. In our case, they signal that the storage is not perfect since some information is carried away by the distorted spin waves and, thus, lost. This is discussed in detail in the next section.

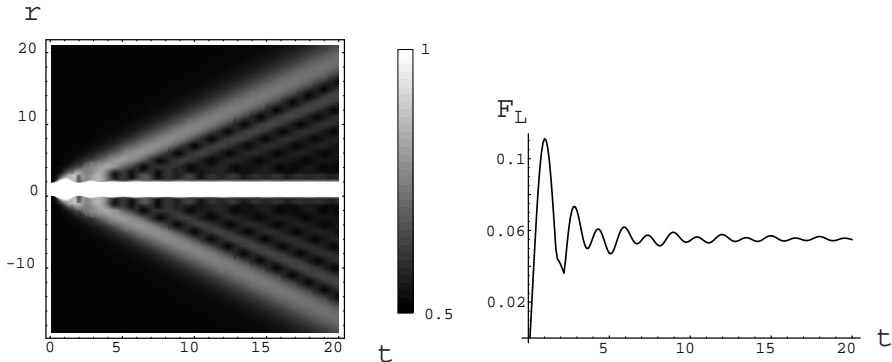


Figure 2.7: Left panel: space-time evolution of the average fidelity F for $\alpha = 3$ with $s = l = 0$. Right panel: time evolution of the leaked fidelity, as defined in Eq. (2.44)

2.7.1 Quality of the Storage

We notice that the loss of information only occurs at short times, while the contribution of the localized state is essentially time independent. This results from the fact that the major component of the initial state is the energy eigenstate $|\Psi_{loc}\rangle$ which does not evolve with time. If the initial state is decomposed as a superposition of energy eigenstates, other contributions are obviously present, but these are propagating states, which leave the defect once and for all after a very short while. These components are small for large α , but nevertheless they are present and give rise to the leakage of information which we describe in the following by introducing two leakage coefficients, valid for the cases of the entanglement and of the single qubit state, respectively.

To characterize the ability to store entanglement at the defect, a leakage coefficient can be designed which quantifies how much can be obtained from other qubits (i.e., the ability to retrieve some entanglement at sites different from l). This can be defined as

$$L := \sum_{r \neq l} C_r^2 \equiv 1 - C_l^2, \quad (2.43)$$

where the second equality comes from the monogamy relation for the pairwise tangles, which in our case gives $\sum_r C_r^2 = 1$, [13].

As shown in the right plot of Figure 2.6, after a transient regime, leakage does not change with time anymore. This agrees with the observation that storage imperfections only occurs at short times while essentially nothing is lost afterwards.

To obtain a similar characterization for the single qubit case, we define a “leaked fidelity”. This is obtained by maximizing the information that can be obtained if one tries to extract the state at a site different from $s = l$:

$$F_L(t) = \max_r \left\{ F_r \right\} - \frac{1}{2}, \quad (2.44)$$

where the term $\frac{1}{2}$, giving the fidelity of the completely mixed state, is subtracted to avoid counting the simple guessing as genuine information retrieval.

This quantity is shown in the right plot of Figure 2.7 and similar considerations apply as those made to comment the behavior of the leakage L .

Indeed, although displaying very different physical quantities, the similarity between Figures 2.6 and 2.7 is quite striking. This results from the nature of the localization process and from the fact that both the fidelity and the concurrence are obtained from the same transition amplitude.

The long time behavior of F_L , however, deserves a comment. One could expect that the quantum information is dispersed all over the chain as time goes on, so that F_L should go to zero. Indeed, this would be the case in the unperturbed problem, in which the dominant long time contribution is $F_L \sim t^{-1/2}$. In the presence of the defect, the decay of F_L saturates. In fact, to understand what is going on, one should look at the position r which realizes the maximum in Eq. (2.44). It turns out that, after a short while, the optimum site is given by the nearest neighbor of the defect. Therefore, what we are effectively looking at is just the tail of the localized state, which, of course, quickly decreases with increasing the defect amplitude α . This is shown in the right plot of Figure 2.8, where the long time behavior of F_L is displayed as a function of α . Notice that the plot starts at $\alpha = 1$, because F_L does not saturate with time for smaller defect strengths. We can also analyze the long time behavior of the entanglement leakage as a function of α . Indeed, L too approaches a finite value for $t \rightarrow \infty$. But the amount of entanglement that can be obtained from other sites goes down as $1/\alpha^2$ (this is easily obtained by using Eq. (2.42) to approximately compute L).

Concerning the localized entanglement, one can also ask which entangled state is effectively stored at the defect. In particular, assuming that the

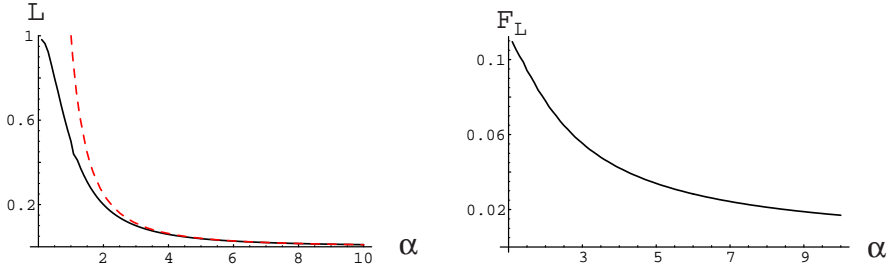


Figure 2.8: Left: long time behavior of the entanglement leakage, displayed as a function of α (solid line). For comparison, the dashed line is a plot of the function $1/\alpha^2$, which approximates L for large values of the defect amplitude. Right: long time values of F_L , plotted with respect to α .

stored state is a superposition of $|01\rangle$ and $|10\rangle$, what is the value of the phase ϕ in the entangled superposition

$$|\Psi^{(\phi)}\rangle = \frac{1}{\sqrt{2}}\left(|01\rangle - e^{i\phi}|10\rangle\right)$$

and what (if any) is the time evolution of ϕ .

To answer this question, we consider the density matrix $\rho^{(2)}$, describing the reduced state of the qubit at the defect site and of the external one. This is the entangled state that is stored in the chain. The concurrence C gives the amount of entanglement present in $\rho^{(2)}$, but does not provide any information about the value of ϕ , which, instead, can be obtained through the function

$$R(\phi) = \langle\Psi^{(\phi)}|\rho^{(2)}|\Psi^{(\phi)}\rangle, \quad (2.45)$$

which returns the degree of resemblance (fidelity) between $\rho^{(2)}$ and the maximally entangled state $|\Psi^{(\phi)}\rangle$. One expects that $R(\phi)$ has a maximum as a function of ϕ , signalling the stored value of the phase. This maximum cannot be exactly 1, since the concurrence itself is not unity. However, as α is increased, $\rho^{(2)}$ becomes more and more pure and we expect $R \rightarrow 1$ for an optimum value of the phase.

Since the localized state has an energy $E_{loc} = -\sqrt{1 + \alpha^2}$, we expect that the time evolving phase factor $e^{-iE_{loc}t}$ is present, so that $R(\phi)$ is a rapidly oscillating function of both α and time. Once this trivial contribution to the phase is subtracted by defining the new variable $\varphi = \phi - E_{loc}t$, a very smooth

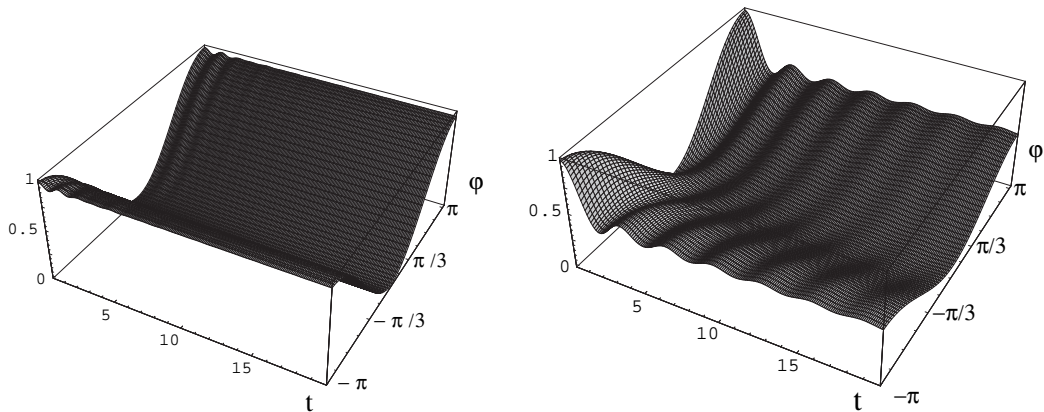


Figure 2.9: The function $R(\varphi)$ (eq.2.45), for $\alpha = 4$ (left) and $\alpha = 0.5$ (right), displayed versus the phase φ and as a function of time.

function $R(\varphi)$ is obtained. This is shown in Figure 2.9 for two values of the defect field.

We are interested in the best value of the phase φ , that is, the value φ_{max} for which R takes its maximum value. If φ_{max} is zero, then the storing preserves the phase of the entangled superposition; whereas a deviation from $\varphi_{max} = 0$ indicates a drift of the phase induced by the chain.

Figure 2.10 shows this maximal phase as a function of α and time. It can be seen that the phase is indeed almost zero, and that small phase drifts are present only for small values of α and at short times (not too short, of course, since at $t = 0$ the phase is fixed to $\varphi_{max} = 0$ by the initial condition).

2.8 Quantum-State Transmission

We now analyze the transmission of a quantum state along the chain when the initial state $|\Psi\rangle$, eq.2.31, doesn't reside on the impurity, whereas, to send entanglement, we choose the spin s in eq.2.35 different from the impurity spin.

The qualitative action of the impurity is to provide a barrier for the propagation of the entanglement wave, fig.2.11, which at the impurity location will be reflected and transmitted by an asymmetrical amount determined by the defect's strength, whereas at all other locations the entanglement spreading is isotropic in both directions. This two features, transmission and

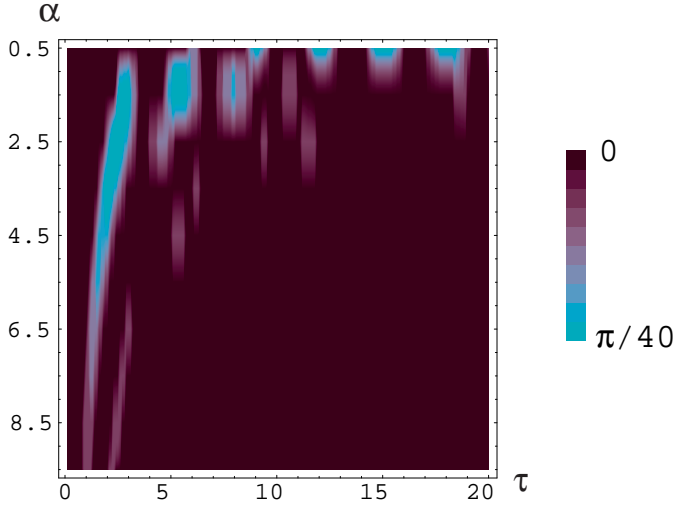


Figure 2.10: The function φ_{max} , as a function of both time and defect strength. One can see that the deviations from zero are quite small and occur at short times and for small defect fields.

reflection of entanglement can be obtained from eq.2.41 which gives for the concurrence:

transmission when sender and receiver are located on opposite sides with respect to l

$$C_r = \frac{1}{2\alpha} (J_{d+1}(t) + J_{d-1}(t))$$

where $d = |r| + |s|$ is the sum of the spin distances from the defect site. This expression shows that the transmission of entanglement through the defect decays also with the impurity level spacing, proportional to α , because the excitation hasn't enough energy to flip the spin and, due to the nearest-neighbors interaction, the excitation cannot reach the spins on the opposite side of s ;

reflection when sender and receiver are on the same side respect to l , (say $r > s > 0$), we have

$$C_r = \left| (-1)^s J_{r-s}(t) - J_{r+s}(t) - i \frac{J_{r+s+1}(t) + J_{r+s-1}(t)}{2\alpha} \right|$$

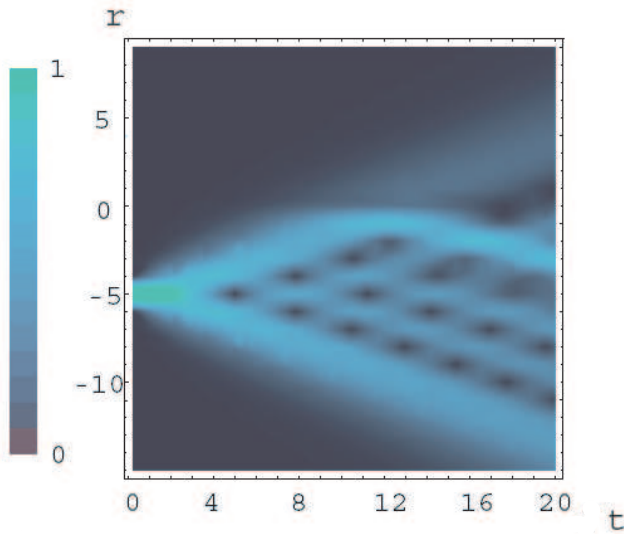


Figure 2.11: time evolution of the concurrence between spin r and the external spin for $\alpha = 2$ when the sender identifies with site $s = -5$. Symmetrical propagation of entanglement up to the impurity site, where backwards reflection occurs, is seen clearly.

where the first term accounts for free entanglement propagation from s to r , the second term represents the reflection of this freely propagating wave, as $r + s$ is the distance traveled from s to $l = 0$ and then to r , while the last term is the amount of entanglement amplitude lost by transmission through the defect. The presence of freely propagating terms can be explained by the small spatial extension of the localized state, which doesn't overlap with the initial state, so that the excitation propagates freely up to the defect, where due to the energy difference, it can neither receive nor transmit forward the reversed spin. As the z component of the total spin has to be conserved, the excitation is reflected backward. Fig.2.11 reports this situation, where, because of the relatively small value of the defect's strength, further order in $\frac{1}{\alpha}$ of eq.2.41 have to be considered and therefore a small amount of transmission of the excitation over the defect site is visible.

To better characterize the effect of the impurity on the entanglement

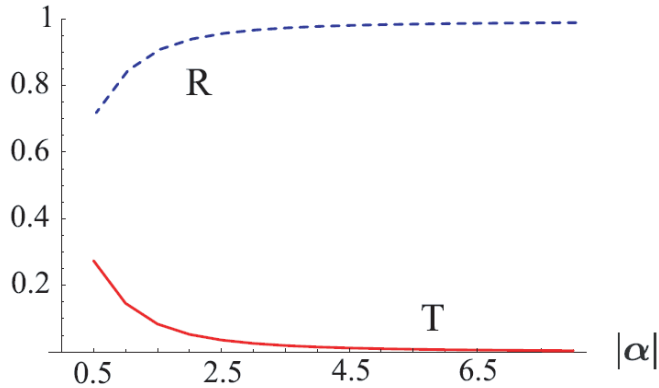


Figure 2.12: transmission and reflection coefficients as defined by eq.2.46. Already for $|\alpha| \geq 5$ an high reflection rate is achieved; for $|\alpha| \rightarrow 0$, instead, the two coefficients approach monotonically $\frac{1}{2}$.

propagation, we introduce the transmission and reflection coefficient observing that single-excitation states saturates the CKW inequality, $\sum_r C_r^2 = 1$. Therefore we assume the tangle as a probability distribution and set

$$T = \lim_{t \rightarrow +\infty} \sum_{r>0} C_r^2 \quad R = \lim_{t \rightarrow +\infty} \sum_{r<0} C_r^2 \quad (2.46)$$

where $s < 0$ has been assumed. One can see that, already for $|\alpha| \leq 5$, transmission coefficient is less than one percent (fig.2.12) and the impurity acts like an entanglement mirror.

2.9 Finite Size Chain

In this section we face the problem of a finite-size chain described by the hamiltonian given by eq.2.9. In fact, this is a more frequently encountered situation (sec.2.2.1), and finite-size considerations are useful for quantum-phase transition characterization, [17].

If the ring is composed of a finite number of spins, the summation in eq.2.23 can't be computed by the integral of eq.2.24; but one can use the

Euler-MacLaurin summation formula [46]

$$\sum_{n=a}^{n=b} f_n = \int_a^b f(x)dx - \frac{1}{2} (f(a) + f(b)) + \sum_{j=1}^{\infty} (-1)^j \frac{B_{2j}}{(2j)!} (f^{(2j-1)}(a) - f^{(2j-1)}(b)) \quad (2.47)$$

where B_j are the Bernoulli numbers, f^j the j -th derivative respect to x , and $f(x)$ the continuous extension of f_n on the real numbers. It's this last condition that doesn't allow the use of this sum rule inside the energy band when applied to Green operator formalism; so only the remaining domain can be investigated. Therefore we can obtain in this section only the energies of the discrete eigenstates (if any) outside the extremes of the one-excitation eigenvalues $\omega_0 \pm 1$, and the corresponding discrete eigenvectors. With the help of eq.2.47 we obtain for the finite-size Green matrix element $G_0^f(n, m; x)$ and for the T^f matrix respectively

$$G_0^f(n, m; x) = G_0(n, m; x) + \frac{(-1)^{|n-m|}}{N(x-1)} \quad (2.48)$$

$$T^f = T + \frac{|l\rangle\langle l|}{N(x-1)} \quad (2.49)$$

where $G_0(n, m; x)$ and T are given by eqs.2.24, 2.25. Also in this case a discrete eigenstate with energy outside the interval $[\omega_0 - 1, \omega_0 + 1]$ arises, given by the solution of cubic equation $y^3 + a_2y^2 + a_1y + a_0 = 0$ with coefficients $a_2 = 2 \left(1 + \frac{\alpha}{N}\right)$, $a_1 = -\alpha^2 + \frac{4\alpha}{N} + \frac{\alpha^2}{N^2}$, $a_0 = \frac{2\alpha^2}{N^2}$ and $y = x - 1$. If we neglect the terms in $\frac{1}{N^2}$, we have a simple quadratic equation, whose solution gives the eigenenergies $E = \omega_0 - \left(\frac{\alpha}{N} \mp \sqrt{1 + \alpha^2 - \frac{2\alpha}{N}}\right)$, with the $+$ sign for $\alpha > 0$ and the $-$ sign otherwise. The corresponding eigenstates, in the computational basis, have the following amplitudes

$$b_n = \frac{\frac{(-x \pm \sqrt{x^2 - 1})^{|n|}}{\pm \sqrt{x^2 - 1}} + \frac{(-1)^{|n|}}{N(x-1)}}{\sqrt{\frac{\pm x}{(x^2 - 1)^{\frac{3}{2}}} + \frac{1}{N(x-1)^2}}} \quad (2.50)$$

where still $x = E - \omega_0$

Even if it is not possible to define a localization length $\xi^f(\alpha)$ like in eq.2.29, the discrete state is localized as the amplitudes are exponentially

decreasing with the distance from the defect, but not-monotonically because of the correction of order $\frac{1}{N}$.

Considering, as in the infinite ring, $\omega_0 > 1$ and α such that the energy of the impurity induced eigenstate becomes the ground state, we quantify the ground-state entanglement between qubit i and j , as usual, by the concurrence $c_{ij} = 2|b_i b_j^*|$, and from the expression of the coefficient amplitudes of eq.2.50, it turns out that, beside localization of entanglement in the neighbourhood of the defect, if one of the spin i or j has an odd lattice distance from the defect, there always exist a couple of values (α, N) for which their entanglement vanishes, fig.2.13. That is due to the fact that the probability amplitude of the i -th site is zero, so for every value of α and N there exist always two spins, equidistant from the defect, who are certainly in the $|0\rangle$ state, thus the ground state has a factorized structure: $|\Psi\rangle = \sum_{n \neq \pm i} b_n |n\rangle \otimes |00\rangle_{+i, -i}$.

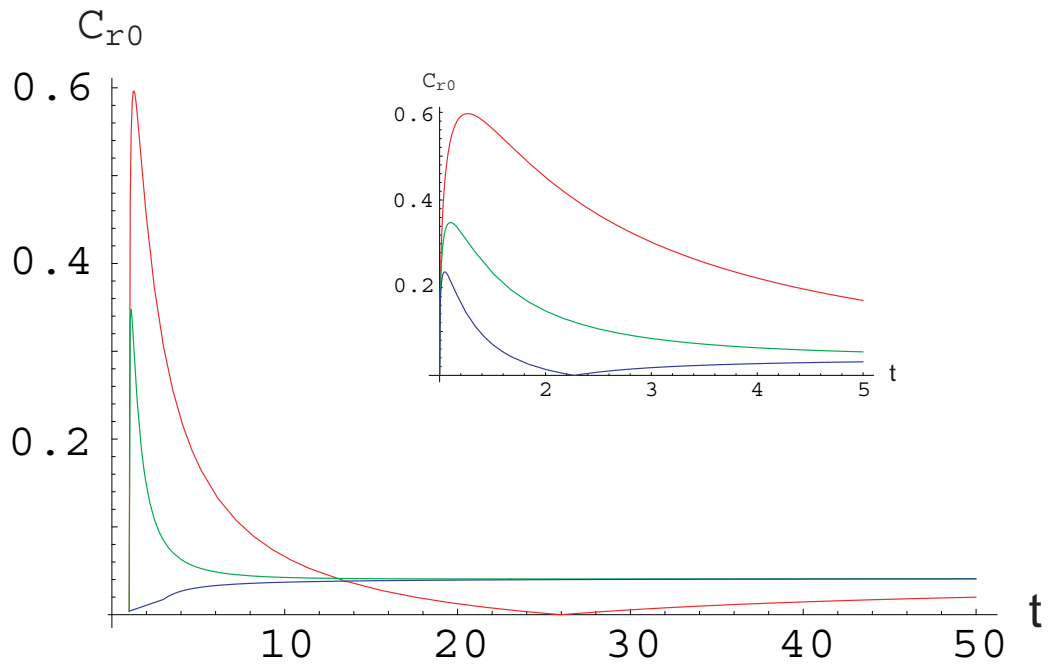


Figure 2.13: ground-state entanglement between spin $i = l = 0$ and spin $r = 1$ (red), $r = 2$ (green) and $r = 3$ (blue) for a spin ring composed of 50 qubits. The concurrence between qubits located at an odd lattice distance from the defect presents a value of α that reduces to zero its entanglement contents. The ground-state entanglement approaches a common finite value for $\alpha \rightarrow \infty$.

Chapter 3

1D Spin Chain with Two Defects

The results of the one-impurity spin ring suggest several modifications of our model in order to accomplish some QIT's tasks. Here we deal with the 1D XX spin ring where one more impurity is added at another site. The reasons for this are:

- the ground-state entanglement in the one-impurity model was localized around the defect site with a spatial extension depending on the defect strength α ; if the number of impurities grows we suppose that more localization points are present, with relative localization ratio depending on the local α 's;
- the possibility of storing quantum states at the impurity site in the one-defect model resides on the Anderson localization around the defect; therefore one could expect that, if the localized states become two, there will be some dynamical effects, such as bouncing entanglement or coherent quantum-state transfer between the two impurity sites, as shown by a perturbative approach in [26];
- the entanglement's reflection at the impurity site is caused by the different qubit level spacing induced there by the inhomogeneity of the magnetic field; therefore providing two different sites with sufficient energy spacing could lead to the possibility of entanglement trapping within the region delimited by the defects.

This chapter is organized as follows: in sec.3.1 the model and its solution is presented, relying on the previously outlined formalism; in sec.3.2 we show the results obtained when the ground state is localized and in the final section we analyze transmission's tasks.

3.1 Hamiltonian

We consider the same hamiltonian as in sec.2.4 but now one more impurity has been added at site m . The hamiltonian describing such a system is

$$H = -\frac{1}{2} \left(\omega_0 \sum_{n=-\frac{N}{2}}^{\frac{N}{2}-1} \sigma_z^n + \sum_{n=-\frac{N}{2}}^{\frac{N}{2}-1} (\sigma_x^n \sigma_x^{n+1} + \sigma_y^n \sigma_y^{n+1}) - \alpha_l \sigma_z^l - \alpha_m \sigma_z^m \right) \quad (3.1)$$

Applying the usual transformations and conventions this hamiltonian becomes

$$H = -\frac{\omega_0}{2} \sum \sigma_z^n - \sum (\sigma_+^n \sigma_-^{n+1} + \sigma_-^n \sigma_+^{n+1}) + \sum_{i=l,m} \frac{\alpha_i}{2} - \sum_{i=l,m} \alpha_i \sigma_+^i \sigma_-^i \quad (3.2)$$

where the un-perturbed system is governed by the first four terms and presents the same solutions as the un-perturbed system of sec.2.4, apart from an additional global energy shift included in the rescaling of the zero-excitation energy $E_0 = 0$. It can be cast also in the form

$$H = -\frac{\omega_0}{2} \sum (|0\rangle\langle 0| - |n\rangle\langle n|) - \sum (|n\rangle\langle n+1| + |n+1\rangle\langle n|) + \frac{\alpha_l + \alpha_m}{2} \sum (|0\rangle\langle 0| + |n\rangle\langle n|) - \alpha_l |l\rangle\langle l| - \alpha_m |m\rangle\langle m| \quad (3.3)$$

which, in the one-excitation sector of the Hilbert space is again, as eq.2.9, equivalent to a tight-binding hamiltonian.

Again the two-impurities model will be solved by use of the Green operator's technique where the role of the un-perturbed hamiltonian in the Dyson series is now played by the one-impurity model and the perturbation is the magnetic field's inhomogeneity α_m on spin m . Again the diagonal form in the one-excitation sector of the Hilbert space allows to re-sum the series and the knowledge of G (or T) permits to solve exactly the eigenvalue problem.

Therefore we use the following notation: the system without impurities has the couple of hamiltonian and Green operator H_0 and G_0 (eq.2.24); with one impurity on site l , H_{0l} and G_{0l} (eq.2.26); whereas the re-summed Dyson series for the Green operator of the full hamiltonian (eq.3.2) becomes

$$G = G_{0l} - G_{0l}R_mG_{0l} \quad (3.4)$$

where $R_m = |m\rangle \frac{\alpha_m}{1 + \alpha_m G_{0l}(m, m)} \langle m|$

After some elementary algebra this expression can be cast in a form where the T matrix is explicitly given

$$T = \frac{|l\rangle t_l \langle l| + |m\rangle t_m \langle m| - |m\rangle t_m G_0(m, l) t_l \langle l| - |l\rangle t_l G_0(l, m) t_m \langle m|}{1 - t_m t_l G_0(m, l) G_0(l, m)}$$

where (see eq.2.25)

$$t_i = \frac{\alpha_i}{1 + \alpha_i G_0(i, i; z)}$$

with $i = l, m$, so that $G = G_0 - G_0 T G_0$.

This can be interpreted using Feynmann diagrams, fig.3.1

The discrete eigenenergies are given by the poles of G (or T), that is by the solution of $1 + \alpha_m G_{0l}(m, m) = 0$; written in terms of $x = E - \omega_0$ one has to solve

$$1 + \alpha_m \left(\frac{1}{\text{Sign}[x] \sqrt{x^2 - 1}} - \frac{\alpha_l (-x + \text{Sign}[x] \sqrt{x^2 - 1})^{2|l-m|}}{(x^2 - 1) \left(1 + \frac{\alpha_l}{\text{Sign}[x] \sqrt{x^2 - 1}} \right)} \right) = 0 \quad (3.5)$$

This equation can be solved analytically for $|l - m| = 1, 2$, i.e. nearest-neighbours and next-nearest neighbours defects.

We focus on the first case, where the analytic expression is simpler and offers a qualitative overview on the physics of the system that holds also for more distant impurities.

The solution of eq.3.5 is given by

$$E = \omega_0 - \frac{2\alpha_l \alpha_m (\alpha_l + \alpha_m) \pm \sqrt{(1 + (\alpha_l - \alpha_m)^2) (1 - 2\alpha_l \alpha_m)^2}}{4\alpha_l \alpha_m - 1}$$

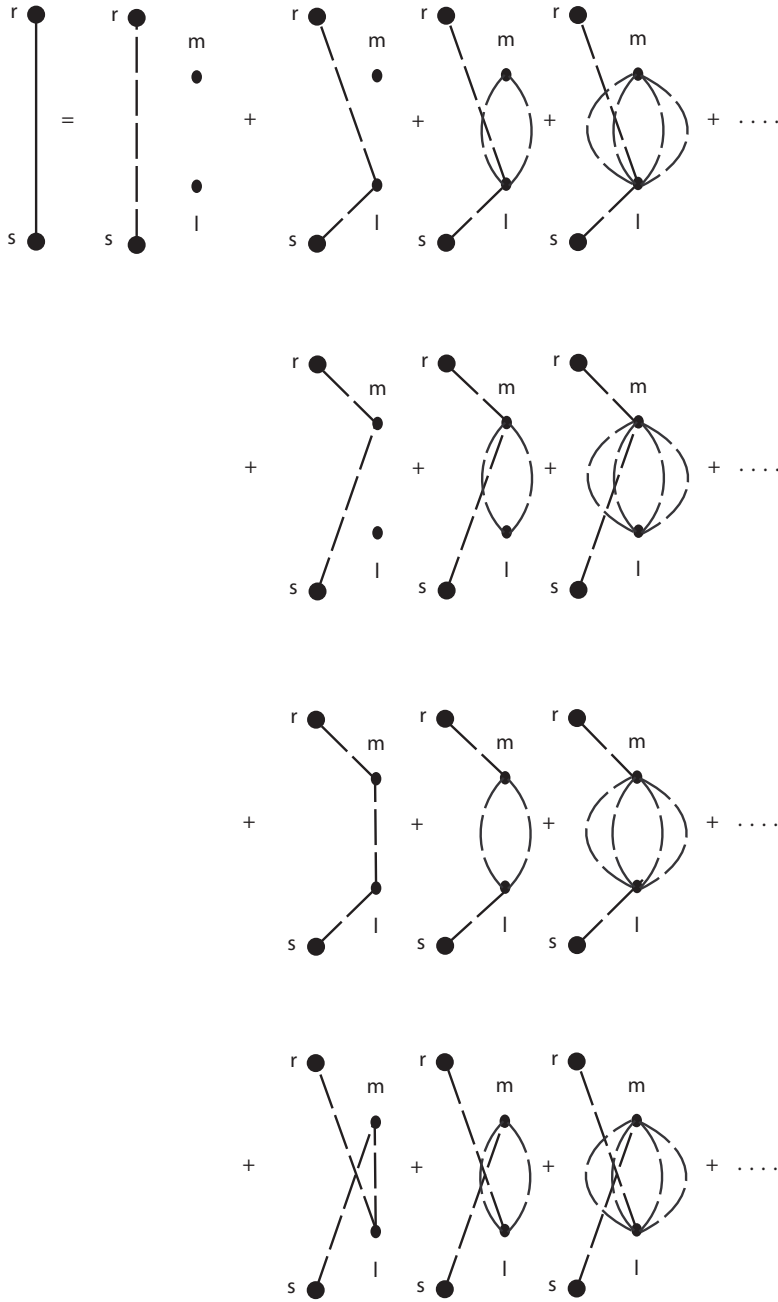


Figure 3.1: The propagator $G(r, s; z)$ is the sum of the free propagation $G_0(r, s; z)$ of the excitation from site s to r , then follow four kind of diagrams. The first (infinite) sum represents $G_0(r, l; z)t_l G_0(l, s; z) + G_0(r, l; z)t_l G_0(l, m; z)t_m G_0(m, l; z)t_l G_0(l, s; z) + \dots$ which gives $\frac{G_0(r, l; z)t_l G_0(l, s; z)}{1 - t_m t_l G_0(m, l) G_0(l, m)}$. Similar considerations apply to the other three series.

These energies must lie outside the energy band, otherwise $G_{0l}(m, m; E)$ would have a non-zero imaginary component; but nevertheless there can be values of $E \in [\omega_0 - 1, \omega_0 + 1]$ such that $Im[G_{0l}(m, m; E')] \simeq 0$ and resonances occur.

Depending on the values of the perturbations, we can have different scenarios, but always at most two simple poles (discrete eigenenergies), which can lie below or above the band.

With reference to fig.3.2(a) the $(\alpha_l \alpha_m)$ plane is divided by four hyperbolae

$$\frac{1}{\alpha_l} + \frac{1}{\alpha_m} = 2 \quad (3.6)$$

$$\frac{1}{\alpha_l} + \frac{1}{\alpha_m} = -2 \quad (3.7)$$

into six areas where different kinds of solutions of eq.3.5 reside.

In the region labelled by 1LB, there's only one solution to eq.3.5 with energy below the band. In fig.3.2(b), $Re[G_{0l}(m, m; E)]$ versus energy E and $\frac{1}{\alpha_m}$ are plotted for $\alpha_l = 0.1$ and $\alpha_m = 2$. The value on the abscissa of the intersection point, according to eq.3.5, gives the energy of the discrete level, E_{loc} . The increase of α_m causes the straight line $\frac{1}{\alpha_m}$ to approach the abscissa, so that still only one intersection point remains, but at more negative energy.

In order to appear a second energy level below the band, the α_l value has to reach the critical value given by eq.3.6. Then the system enters the region denoted by 2LB, and from fig.3.2(c), plotted for $\alpha_l = 1$ and $\alpha_m = 2$, one sees that the change of the α_m value affects both energy levels.

If, instead, α_m has a negative value, the system can enter the (1LA, 1LB) region by crossing the hyperbolae given by eq.3.7, where one level is above the energy band while the other is below. This is also the case reported in fig.3.2(d), with $\alpha_l = \frac{1}{2}$ and $\alpha_m = -2$.

Similar consideration applies to the other regions of fig.3.2(a).

If the distance between the defects in the spin ring augments, the hyperbolae approach more and more the $\alpha_l \alpha_m$ axis, but the outlined qualitative features still hold.

Denoting the eigenenergy with $x = E - \omega_0$, the corresponding discrete eigenstate, given in the computational basis $|\Psi_L\rangle = \sum_n b_n |n\rangle$, has the fol-

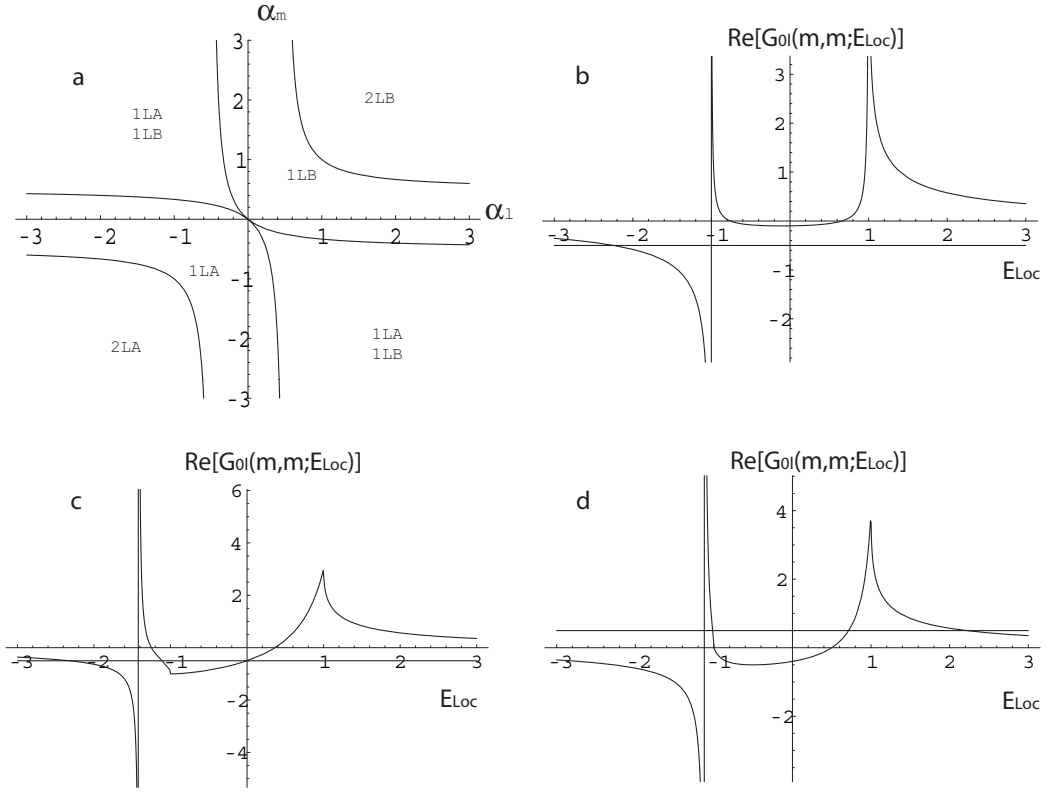


Figure 3.2: (a) the hyperbolas divide the (α_l, α_m) -plane in six different regions: one or two levels above the unperturbed energy band (1LA, 2LA), one or two levels below (1LB, 2LB) or one level above (1LA) and another below (1LB); the remaining three figures show the plot of $\text{Re}[G_{0l}(m, m; E)]$ versus energy E and $\frac{1}{\alpha_m}$ for nearest-neighbour impurity sites. The abscissa coordinate of their intersection point(s) gives the solution of eq.3.5, indicating therefore the energy of the discrete eigenstate(s). (b) $\alpha_l = 0.1$ and $\alpha_m = 2$: there's only one level below the energy band, represented by the $[-1, 1]$ interval on the abscissa; (c) $\alpha_l = 1$ and $\alpha_m = 2$: two levels below; (d) $\alpha_l = \frac{1}{2}$ and $\alpha_m = -2$: one level above and another below the energy band.

lowing amplitudes

$$b_n = \frac{G_{0l}(n, m; x)}{\sqrt{-G'_{0l}(m, m; x)}} \quad b_n = \text{cost} (e^{-\xi(|n-l|)} + K e^{-\xi(|n-m|)}) \quad (3.8)$$

Also in this case the discrete eigenstate(s) are localized around the two defect sites, with inverse localization length given by the same function as the one-impurity model $\xi(E) = -\ln(-x + \sqrt{x^2 - 1})$, and with a coefficient $K = K(\alpha_l, \alpha_m)$ that accounts for the ratio of the amplitude coefficients of finding the excitation on site l or m ; so that for $\alpha_l = \alpha_m$ we have $K = \pm 1$. It is interesting to note that expression 3.8 give rise to eigenstate(s) representing a coherent superposition of $|l\rangle$ and $|m\rangle$ for large enough α 's.

Moreover, for equal and large enough α 's, two localized eigenstates appear, which can be cast in the following useful form

$$|\Psi(\omega_1)\rangle = \frac{1}{\sqrt{2}} (|l\rangle + |m\rangle) \quad (3.9)$$

$$|\Psi(\omega_2)\rangle = \frac{1}{\sqrt{2}} (|l\rangle - |m\rangle) \quad (3.10)$$

If, on the other hand, only one level appears by taking $\alpha_l = \alpha_m$, it's the first expression that holds.

The additional impurity, as in the one-defect model, doesn't change the energy band, because the branch cut of the Green function for the two-defect model is still determined by the unperturbed Green function.

Referring to the eigenstates within the energy band, we obtain, applying $|\Psi_E\rangle = |\phi\rangle + G_0^+ T^+ |\phi\rangle$, the following expression for the a_n 's in the computational basis expansion $|\Psi(E)\rangle = \sum a_n |n\rangle$:

$$a_n = \frac{1}{\sqrt{N}} \left(\frac{e^{in\theta} + \frac{g_{nl}^+(\alpha_l) e^{i\theta} + g_{nm}^+(\alpha_m) e^{im\theta} + g_{nm}^+(\alpha_m) g_{ml}^+(\alpha_l) e^{i\theta} + g_{nl}^+(\alpha_l) g_{lm}^+(\alpha_m) e^{im\theta}}{1 - g_{ml}^+(\alpha_m) g_{lm}^+(\alpha_l)}} \right)$$

where $g_{nl}^+(\alpha_i)$'s are defined by eq.2.40 with α_i set to α_l or α_m .

It is easy to verify that if one of the α 's becomes 0 we return to the single defect case.

3.2 Ground-State Entanglement

Choosing the values of α 's such that the localized state becomes the ground state, a non-zero pairwise entanglement between spins in the neighbourhood

of the defects appears. That means that, as in the one-defect model, a first-order quantum phase transition occurs and the new ground state exhibits a ground-state entanglement structure.

$$C_{ij}(|\Psi_{loc}(E_{loc})\rangle) = 2|Res(G(i, j; E_{loc}))| \equiv 2|b_i^{loc}b_j^{loc*}| \quad (3.11)$$

It's expression in terms of Green's function is

$$C_{ij} = 2 \left| \frac{(G_0(i, m) + t_l G_0(l, m) G_0(i, l)) (G_0(m, j) + t_l G_0(m, l) G_0(l, j))}{-G'_{0l}(m, m)} \right|$$

Referring to eq.3.11 and, for equal and large enough positive α 's, using eq.3.9, two-party entanglement is present also in the limit $\alpha \rightarrow \infty$, but only between the two impurities and has the value of $C_{lm} = 1$. This didn't occur in the one-model defect, where the ground state was factorized both in the $\alpha = 0$ and in the $\alpha \rightarrow \infty$ case. The reason is that the impurity tends to entangle with the lattice sites within the localization length ξ , but, as this becomes less than the lattice spacing, the whole ring is left in a product state between a Bell state, involving the two impurities, and the rest of the chain in the zero-excitation sector of Hilbert space:

$$|\Psi_{GS}\rangle \rightarrow \frac{1}{\sqrt{2}} (|1_l 0_m\rangle + |0_l 1_m\rangle) \otimes |0\rangle$$

If the ground state belongs to the region $\alpha_l, \alpha_m > 0$ of fig.3.2, then two localization points appear in the spin ring; in the sense that every qubit is entangled with both impurities, with the entanglement between the qubit and the impurity on which α is greater being higher than the entanglement with the other impurity. Moreover, if the defect's strength reduces on one of the impurity, so does entanglement between this impurity site and a qubit of the ring; in the meanwhile entanglement between the same qubit and the other impurity grows.

It is also possible to have a localized ground state with one of the α 's negative, if on the other impurity site there's a sufficiently high positive magnetic field. In that case the negative-valued impurity site is only weakly entangled, and it's entanglement amount can be made arbitrarily small by reducing further its defect strength.

Analyzing the various cases we can have (fig.3.2):

$\alpha_l = \alpha_m$ From eqs.3.11 and 3.8, we obtain that for every spin i , $C_{il} = C_{im}$ regardless of site distances between the spin involved (fig.3.2(a)). In particular, looking at the entanglement between distant defects, it can also reach considerably high values (fig.3.2(b));

$\alpha_l > \alpha_m > 0$ The ground state entanglement between every spin i and l exceeds that one with m , because the amplitude coefficient $b_l > b_m$, also if spin i is nearer to m than to l , $|m - i| < |l - i|$ (fig.3.2(c));

$\alpha_l > 0, \alpha_m < 0$ The entanglement of i with l grows by lowering α_m , while, on the other hand, entanglement between i and m decreases, and, at the same time, entanglement between i and the spins located on the opposite side with respect to m is highly suppressed (fig.3.2(d)).

All these properties suggest the possibility to control bipartite ground-state entanglement between spins acting on a remote third party, as well as the possibility to entangle definite spins in the ring simply by introducing magnetic inhomogeneities on them.

3.3 Quantum-State Transmission

As we investigate in this section the role of the defects on the QIT's tasks described in sec.2.6, we can use the same expressions for the fidelity (eq.2.34) and the concurrence (eq.2.37), because the additional defect doesn't change the structure of the density matrix; therefore the quantity of interest is the transition amplitude $f_{rs}(t) = \langle r|H|s \rangle$, which has the same analytical structure than the one-defect model (eq.2.39), apart from an eventually additional localized state. Also the same considerations apply to the interpretation of its expression

$$f_{rs}(t) = \sum_{E_{loc}} e^{iE_{loc}t} \text{Res} (G(r, s; E_{loc})) + \int_{-\pi}^{\pi} \frac{d\theta}{2\pi} e^{-iEt} \quad (3.12)$$

$$\left(e^{ir\theta} + \frac{G_0^+(r,l)t_l e^{i\theta} + G_0^+(r,m)t_m e^{im\theta} + G_0^+(r,m)t_m G_0^+(m,l)t_l e^{i\theta} + G_0^+(r,l)t_l G_0^+(l,m)t_m e^{im\theta}}{1 - t_l t_m G_0^+(l,m) G_0^+(m,l)} \right)$$

$$\left(e^{is\theta} + \frac{G_0^+(s,l)t_l e^{i\theta} + G_0^+(s,m)t_m e^{im\theta} + G_0^+(s,m)t_m G_0^+(m,l)t_l e^{i\theta} + G_0^+(s,l)t_l G_0^+(l,m)t_m e^{im\theta}}{1 - t_l t_m G_0^+(l,m) G_0^+(m,l)} \right)^*$$

To discuss the main features that appear in the entanglement distribution, we consider two cases:

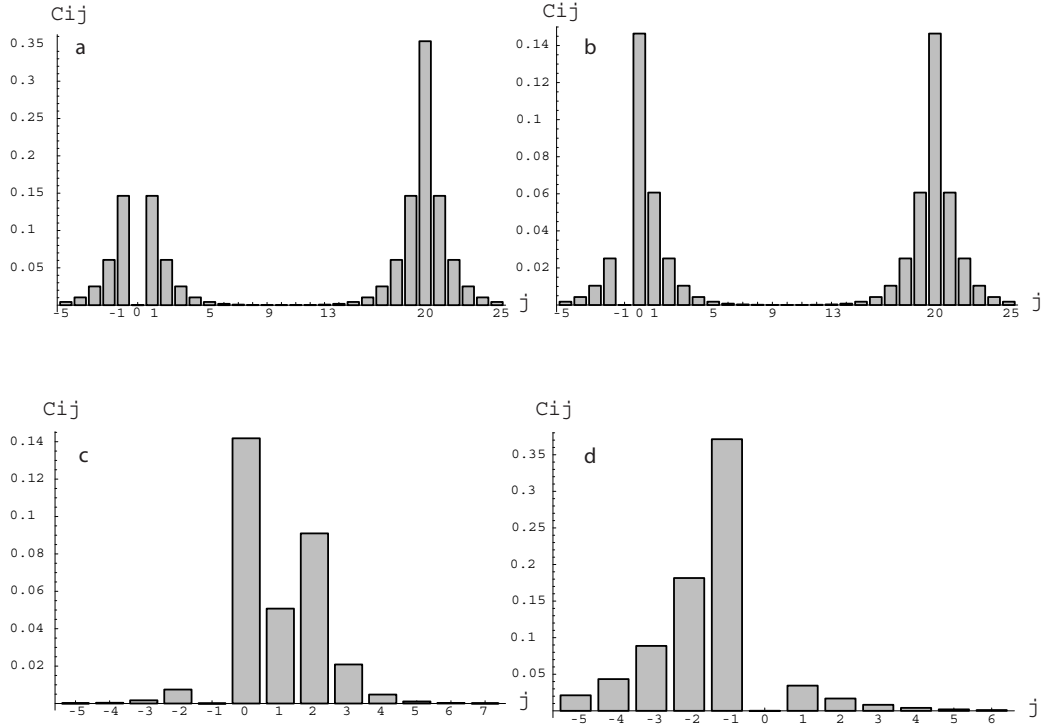


Figure 3.3: ground state entanglement between a fixed spin i and a spin j on different lattice sites: (a) $i = 0$, $\alpha_l = \alpha_m = 1$, $l = 0$ and $m = 20$ - the impurity spin l presents entanglement, spatially localized, not only with the spins around itself, but also with the impurity on a distant site m and the spins in its neighbourhood; (b) $i = -1$, $\alpha_l = \alpha_m = 1$, $l = 0$ and $m = 20$ - the entanglement contents between an arbitrary spin and one of the impurity equals the entanglement with the other impurity, the same consideration applies to its entanglement with the spins having the same lattice distance from one or another defect; (c) $i = -1$, $\alpha_l = 2$, $\alpha_m = 1.9$, $l = 0$ and $m = 2$ - lowering the value of the impurity on site m reduces its entanglement contents as well as those of its neighbour spin; (d) $i = 0$, $\alpha_l = 1$, $\alpha_m = -10$, $l = 0$ and $m = 1$ - for negative values of the defect's strength on site m , its concurrence is highly suppressed, whereas the concurrence of the other impurity spin has been enhanced.

entanglement bouncing In reference to fig.3.4, we consider an initial state $|\Psi(0)\rangle = \frac{1}{\sqrt{2}}(|0_x 1_l\rangle - |1_x 0_l\rangle)|0\rangle$, that is a singlet state between the external spin x and one of the impurities, say l , has been realized. Then the system evolves and it turns out that entanglement between the external spin and those belonging to the chain involves only the impurities. The dynamics shows oscillatory maximal entanglement transfer, i.e. $C_{xi} = 1$, between the external spin and alternatively each impurity at a rate inversely proportional to the frequency separation of the two localized levels. This can be understood observing that, for identical defect intensities, the discrete states are equally like localized around l and m , so that, using eq.3.9, we can write

$$|l\rangle = \frac{1}{2}(|\Psi_1\rangle + |\Psi_2\rangle) \quad |m\rangle = \frac{1}{2}(|\Psi_1\rangle - |\Psi_2\rangle)$$

and all concurrences, except C_{xl} and C_{xm} , are zero, because all amplitudes, except b_l and b_m , are zero in the expansions of the $|\Psi_i\rangle$'s. Finally the oscillatory behaviour of concurrence is obtained using eq.3.12

$$C_{lx} = \frac{1}{2} \left| e^{-iE_{loc}^{(1)}t} + e^{-iE_{loc}^{(2)}t} \right| \quad C_{mx} = \frac{1}{2} \left| e^{-iE_{loc}^{(1)}t} - e^{-iE_{loc}^{(2)}t} \right| \quad (3.13)$$

where $E_{loc}^{(i)}$ refers to the energy of the i -th discrete level. If we choose $(E_{loc}^{(1)} + E_{loc}^{(2)})/2$ as the zero of the energy scale (or, equivalently, multiply by a irrelevant phase factor $e^{i(E^{(2)} - E^{(1)})/2}$), eq.3.13 can be re-written as

$$C_{lx} = \cos(\omega_{21}t) \quad C_{mx} = \sin(\omega_{21}t)$$

where ω_{21} is the Rabi frequency $(E_2 - E_1)/2$. This could lead to long-distance transfer of entanglement simply by putting the impurities far away each other; unfortunately the energy difference of the two localized eigenstates approaches rapidly zero with increasing distances so one would have to wait a considerably long time ($t = \frac{\pi}{\omega_{21}}$) just to obtain the first peak in fig.3.4;

entanglement trapping In reference to fig.3.5, we consider the situation where the sender s is equidistant from the two equal-strength impurities. From an qualitative point of view, the reflected entanglement waves recombine coherently at the sender site, while the transmitted ones go over the rest of the chain. Augmenting the defects strengths

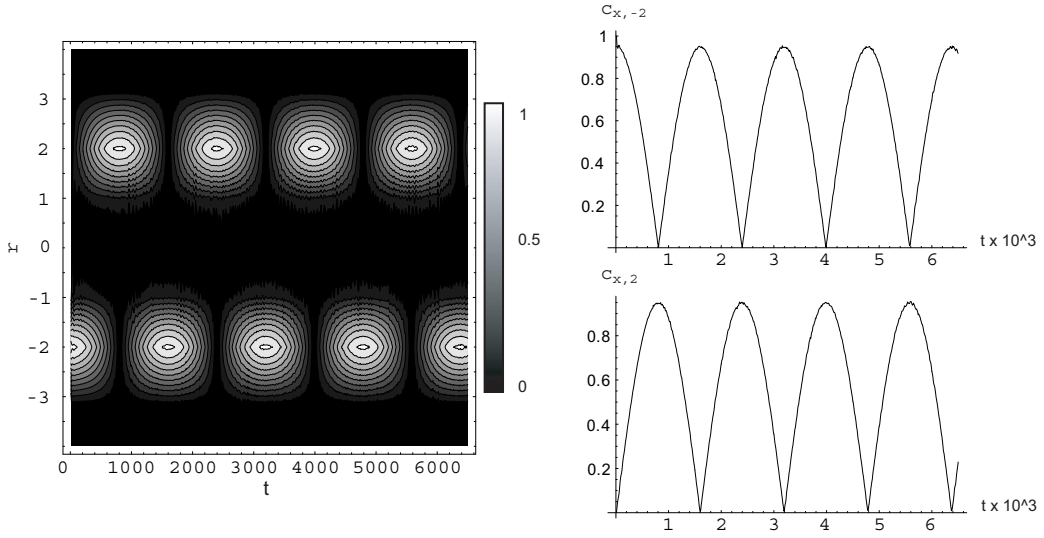


Figure 3.4: concurrence between an external spin and spin r with $s = -2$, $\alpha_l = \alpha_m = 3$, $l = -2$ and $m = 2$: (left) entanglement bounces only between the two impurities, with the other spins uncoupled from the dynamics; (right) concurrence of each impurity with the external spin x exhibits Rabi oscillations with frequency given by the energy difference between the two localized levels.

and placing the impurities on both sides of the sender, almost total reflection can be achieved. Therefore, in fig.3.5(a), the slope of concurrence's envelope approaches the abscissa, and entanglement turns out to be trapped on the sender site; at the same time, the entanglement shared by the defect (fig.3.5(b)) and that transmitted over the rest of the chain (fig.3.5(c)) reduce to zero.

If we augment the distance of the impurities from the sender site (fig.3.6), the entanglement propagates almost freely in the region bounded by the two defects, wherein interference effects can account also for a revival of entanglement on the sender site (fig.3.6 (a))

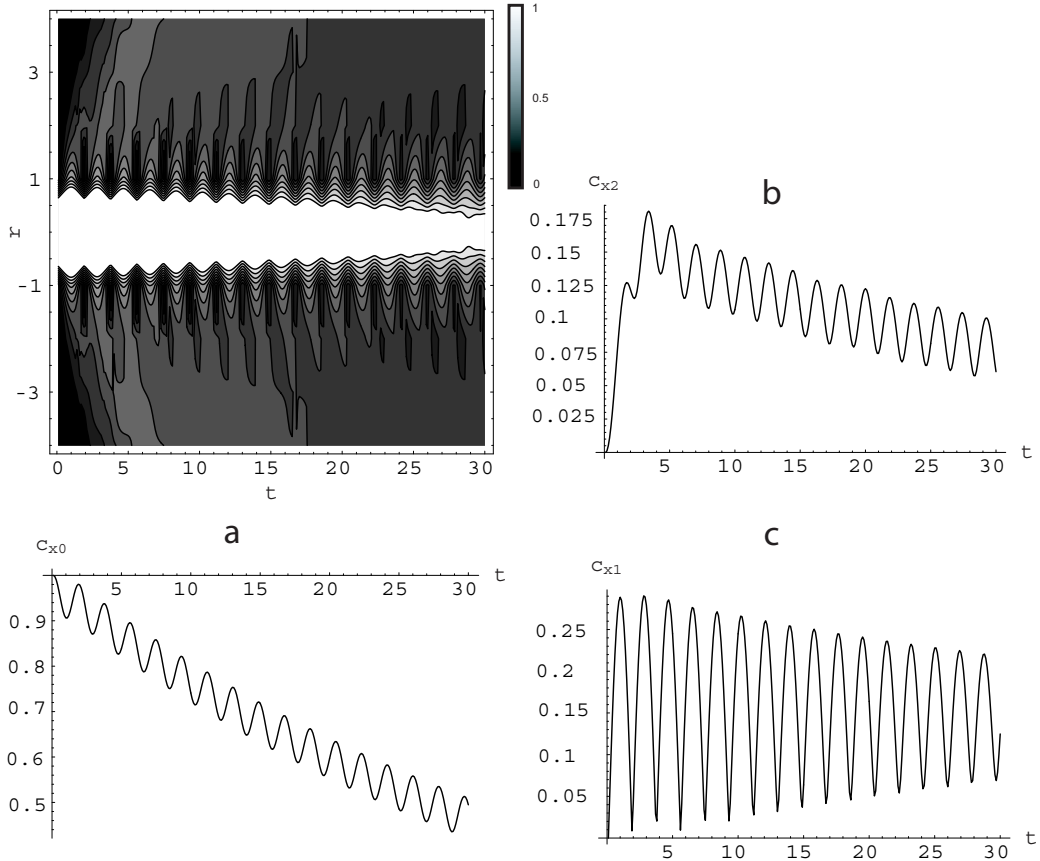


Figure 3.5: concurrence between an external spin x and spin r with $s = 0$, $\alpha_l = \alpha_m = 3$, $l = -1$ and $m = 1$; (a) the initial entanglement between spin s and the external one x tends to remain localized because the next-neighbours impurity cannot accept the excitation; (b) and (c) show the concurrence with the impurity and spin $r = 2$.

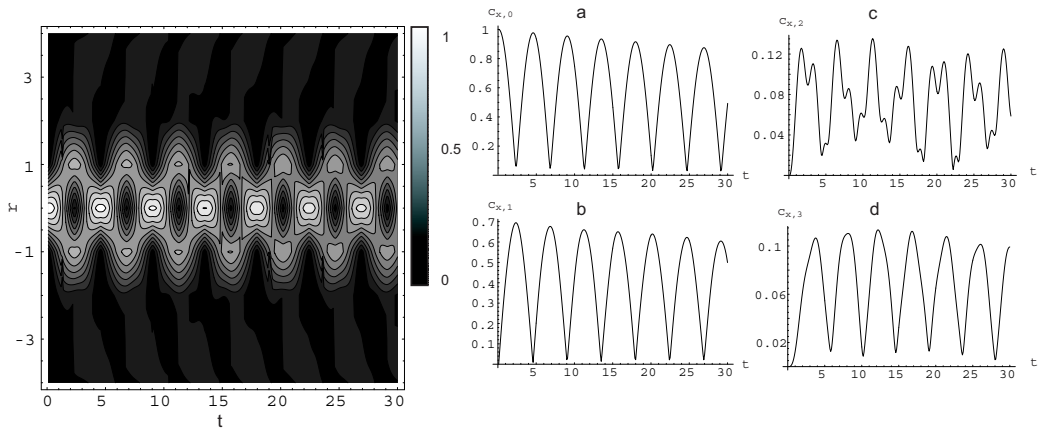


Figure 3.6: left: concurrence between an external spin and spin r with $s = 0$, $\alpha_l = \alpha_m = 3$, $l = -2$ and $m = 2$; (a) concurrence of spin 0 where the peaks are due to the constructive interference of the entanglement waves, (b) concurrence of spin 1 whose maximum correspond to the minimum of the concurrence in fig.(a), because perfect entanglement transfer is possible in a three-qubit chain; (c) and (d) concurrence of the defect and spin 3 accounting for the entanglement's transmission over the defect (which in the limit $\alpha \gg 1$ would be zero)

Conclusions

In this thesis we have studied the effects on ground-state entanglement and quantum-state transfer caused by the presence of one and two diagonal impurities in a 1D ring-shaped spin- $\frac{1}{2}$ hamiltonian with XX ferromagnetic coupling placed in an otherwise homogeneous transverse magnetic field. We have restricted our attention to the one-excitation sector of the Hilbert space, where the hamiltonian becomes equivalent to a tight-binding model. In both cases, Schrödinger equation has been solved exactly via Green's operator formalism.

In the one-impurity model the presence of the defect causes a first order quantum phase transition, where the new ground state of the system becomes localized around the impurity site. In this state bipartite entanglement is different from zero for spins in a region contained within a localization length, which depends on the ratio of the magnetic inhomogeneity and the exchange coupling (α).

We have also analyzed the transmission of quantum information along such a chain. We have found that the presence of the defect is responsible of various phenomena: 1.) information storage: if the state is encoded initially in the impurity, it doesn't diffuse away and both fidelity and concurrence retain its initial maximum value; 2.) mirror effect: if the state isn't encoded initially in the defect, entanglement waves get reflected and transmitted at the impurity site by an amount depending on reflection and transmission coefficients, where, they too, involve the same ratio.

In the two-impurity model, a similar quantum phase transition occurs, and ground-state entanglement becomes localized too, with the same functional relation for the localization length as in the one-impurity model. Nevertheless in this case two localization points arise in the spin ring. Quantum-state transfer, in the limit of $\alpha \gg 1$, exhibits : 1.) bouncing effect: if the initial singlet state involves one of the impurities and the external spin, en-

tanglement bounces between the defects with Rabi oscillations of frequency given by the energy difference of the two localized eigenstates; 2.) entanglement trapping: relying on the mirror effect of the two impurities, the entanglement waves remain confined into the region delimited by the defects sites.

From an experimental point of view, we have presented a model that permits to achieve quantum information tasks by systems realizable with present-day technology and requiring minimum control operations. Further studies (inclusion of dynamical properties of the impurities, characterization of the quantum phase transition from an q-information point of view, extension to higher spatial dimensionality and/or other sectors of the Hilbert space, entanglement versus disorder, etc.) should be give more insight on the fundamental physics behind entanglement's theory as well as suggest some achievable experimental protocols for quantum information development.

The author wishes to thank the Quantum Information Theory Group at the Dept. of Physics - University of Calabria: Prof. G. Falcone, Prof. F. Piperno, Dr. F. Plastina, Dr. A. Sindona, Dr. G. Liberti, Dr. R.L. Zaffino and Dr. F. Francica without whom this work wouldn't have been realized.

Bibliography

- [1] Michael A. Nielsen and Isaac L. Chuang. *Quantum Computation and Quantum Information*. Cambridge University Press, 2000.
- [2] John Preskill. Lecture notes for physics 229: Quantum information and computation. URL:<http://theory.caltech.edu/people/preskill/ph229/>, 1998.
- [3] Asher Peres. *Quantum Theory: Concepts and Method*. Kluwer Academic Publishers, 2002.
- [4] N. Rosen A. Einstein, B. Podolsky. Can quantum-mechanical description of physical reality be considered complete? *Phys. Rev.*, 47:777, 1935.
- [5] John S. Bell. On the einstein podolsky rosen paradox. *Physics*, 1:195, 1964.
- [6] John F. Klauser et al. Proposed experiment to test local hidden-variable theories. *Phys. Rev. Lett.*, 23(15):880, 1969.
- [7] Daniel Rohrlich Sandu Popescu. Thermodynamics and the measure of entanglement. *Phys. Rev. A*, 56(5):R3319, 1997.
- [8] Charles H. Bennet. Concentrating partial entanglement by local operations. *Phys. Rev. A*, 53(4):2046, 1996.
- [9] Reinhard W. Bell. Quantum states with einstein-podolsky-rosen correlations admitting a hidden-variable model. *Phys. Rev. A*, 40(8):4277, 1989.
- [10] Wootters W. K. Entanglement of formation of an arbitrary state of two qubits. *Phys. Rev. Lett.*, 80:2245, 1998.

- [11] Pranaw Rungta et al. Universal state inversion and concurrence in arbitrary dimensions. *Phys. Rev. A*, 64:042315, 2001.
- [12] G. Vidal W. Dür and J.I.Cirac. Three qubits can be ebtangled in two inequivalent ways. *quant-ph/0005115*, 2006.
- [13] William K. Wootters Valerie Coffman, Joydip Kundu. Distributed entanglement. *Phys. Rev. A*, 61:052306, 2000.
- [14] Stephen J. Wiesner Charles H.Bennet. Communication via one- and two-particle operators on einstein-podolsky-rosen states. *Phys. Rev. Lett.*, 69(20):2881, 1992.
- [15] C. H. Bennett et al. Teleporting an unknown quantum state via dual classical and einstein-podolsky-rosen channels. *Phys. Rev. Lett.*, 70:1895, 1993.
- [16] Michael A. Nielsen Tobias J. Osborne. Entanglement in a simple quantum phase transition. *Phys. Rev. A*, 66:032110, 2002.
- [17] A. Osterloh et al. Scaling of entanglement close to a quantum phase transition. *Nature*, 416:608, 2002.
- [18] Sougato Bose. Quantum communication through an unmodulated spin chain. *Phys. Rev. Lett.*, 91(20):207901, 2003.
- [19] Rosario Fazio Alessandro Romito and C. Bruder. Solid-state quantum communication with josephson arrays. *Phys. Rev. B*, 71:100501R, 2005.
- [20] M. Paternostro et al. Quantum state transfer in imperfect artificial spin networks. *Phys. Rev. A*, 71:042311, 2005.
- [21] M.A. Martìn-Delgado F. Verstraete and J.I. Cirac. Diverging entanglement length in gapped quantum spin systems. *Phys. Rev. Lett.*, 92(8):087201, 2004.
- [22] Daniel Burgarth and Sougato Bose. Conclusive and arbitrarily perfect quantum-state transfer using parallel spin-chain channels. *Phys. Rev. A*, 71:052315, 2005.

- [23] Vittorio Giovannetti and Daniel Burgarth. Improved transfer of quantum information using a local memory. *Phys. Rev. Lett.*, 96:030501, 2006.
- [24] Christandl M. et al. Perfect state transfer in quantum spin networks. *Phys. Rev. Lett.*, 92:187902, 2004.
- [25] Gabriele De Chiara et al. From perfect to fractal transmission in spin chains. *Phys. Rev. A*, (72):012323, 2005.
- [26] L.F. Santos. Entanglement in quantum computer described by the xxz model with defects. *Phys. Rev. A*, 67:062306, 2003.
- [27] L.F. Santos and G. Rigolin. Effects of interplay between interaction and disorder in bipartite entanglement. *Phys. Rev. A*, 71:032321, 2005.
- [28] L.F. Santos et al. Strong many-particle localization and quantum computing with perpetually coupled qubits. *Phys. Rev. A*, 71:012317, 2005.
- [29] Zhen Huang Omar Osenda and Sabre Kais. Tuning the entanglement for a one-dimensional magnetic system with anisotropic coupling and impurities. *Phys. Rev. A*, 67:062321, 2003.
- [30] G. Rigolin L.F. Santos and C.O. Escobar. Entanglement versus chaos in disordered spin chains. *Phys. Rev. A*, 69:042304, 2004.
- [31] P.W. Anderson. Absence of diffusion in certain random lattices. *Phys. Rev.*, 109(5):1492, 1958.
- [32] Economou E. N. *Green's Function in Quantum Physics*. 2nd edition, 1983.
- [33] Gerald D. Mahan. *Many-particles physics*. Plenum Press, 2nd edition, 1990.
- [34] Alexei M. Tsvelik. *Quantum Field Theory in Condensed Matter Physics*. Cambridge University Press, 2003.
- [35] Eduardo Fradkin. Jordan-wigner transformation for quantum-spin systems in two dimensions and fractional statistics. *Phys. Rev. Lett.*, 63(3):322, 1989.

- [36] Luis Huerta and Jorge Zanelli. Bose-fermi transformation in three-dimensional space. *Phys. Rev. Lett.*, 71(22):3622, 1993.
- [37] B.D. Josephson. The discovery of tunneling supercurrents. *Rev. Mod. Phys.*, 46(2):251, 1974.
- [38] D. Vion et al. Manipulating the quantum state of an electrical circuit. *Science*, 296:886, 2002.
- [39] R. Fazio C. Bruder and G. Schön. Superconductor-mott-insulator transition in bose systems with finite-range interactions. *Phy. Rev. B*, 47(1):342, 1993.
- [40] D. Jaksch and P. Zoller. The cold atom hubbard toolbox. *Annals of Physics*, 315:52, 2005.
- [41] Andreas Osterloh Luigi Amico and Francesco Cataliotti. Quantum many particles systems in ring-shaped optical lattices. *Phys. Rev. Lett.*, 95:063201, 2005.
- [42] P.M. Platzman and M.I. Dykman. Quantum computing with electrons floating on liquid helium. *Science*, 284:1967, 1999.
- [43] Amico L. et al. Dynamics of entanglement in one-dimensional spin systems. *Phys. Rev. A*, 69:022304, 2004.
- [44] Francesco Plastina et al. Spin wave contribution to entanglement in heisenberg models. *New J. Phys.*, 6:124, 2004.
- [45] Z. Song and C.P. Sun. Quantum information storage and state transfer based on spin systems. *Low Temp. Phys.*, 31(8):686, 2005.
- [46] Stegun I.A. Abramowitz M. *Handbook of Mathematical Functions*. Dover Publications, Inc., New York, 1970.